Lithium suppression of tau induces brain iron accumulation and neurodegeneration

DOI:
10.1038/mp.2016.96

Document Version
Accepted author manuscript

Lithium suppression of tau induces brain iron accumulation and neurodegeneration

Peng Lei[1,2,*], Scott Ayton[2], Ambili Thoppuvalappil Appukuttan[2], Steve Moon[2], James A. Duce[2,3], Irene Volitakis[2], Robert Cherny[2], Stephen J. Wood[4,5], Mark Greenough[2], Gregor Berger[6,7], Christos Pantelis[2,4,8], Patrick McGorry[6], Alison Yung[9], David I. Finkelstein[2], and Ashley I. Bush[2,*]

[1] Department of Neurology, State Key Laboratory of Biotherapy, West China Hospital, Sichuan University, and Collaborative Innovation Center for Biotherapy, Sichuan, China

[2] Florey Institute of Neuroscience and Mental Health, The University of Melbourne, Parkville, Victoria, Australia

[3] School of Biomedical Sciences, Faculty of Biological Sciences, University of Leeds, West Yorkshire, United Kingdom

[4] Melbourne Neuropsychiatry Centre, Department of Psychiatry, University of Melbourne, and Melbourne Health, Victoria, Australia

[5] School of Psychology, University of Birmingham, Birmingham, UK

[6] ORYGEN Research Centre, University of Melbourne and Melbourne Health, Victoria, Australia

[7] University of Zürich, Department of Child and Adolescent Psychiatry, Zurich, Switzerland

[8] Centre for Neural Engineering, Department of Electrical and Electronic Engineering, University of Melbourne, Parkville, Victoria, Australia

[9] Institute of Brain, Behaviour and Mental Health, University of Manchester and Greater Manchester West NHS Mental Health Trust, Manchester, UK

*Correspondence to

Dr. Peng Lei, peng.lei@scu.edu.cn; peng.lei@florey.edu.au

Or

Prof. Ashley I. Bush, ashley.bush@florey.edu.au

Running Title: Lithium elevates brain iron via tau

Abstract

Lithium is a first-line therapy for bipolar affective disorder. However, various adverse effects, including a Parkinson-like hand tremor, often limit its use. The understanding of the neurobiological basis of these side effects is still very limited. Nigral iron elevation is also a feature of Parkinsonian degeneration, which may be related to soluble tau reduction. We found that MRI T_2 relaxation time changes in subjects commenced on lithium therapy were consistent with iron elevation. In mice, lithium treatment lowers brain tau levels and increases nigral and cortical iron elevation that is closely associated with neurodegeneration, cognitive loss and parkinsonian features. In neuronal cultures lithium attenuates iron efflux by lowering tau protein, which traffics amyloid precursor protein to facilitate iron efflux. Thus, tau- and APP- knockout mice were protected against lithium induced iron elevation and neurotoxicity. These findings challenge the appropriateness of lithium as a potential treatment for disorders where brain iron is elevated (e.g. Alzheimer's disease), and may explain lithium-associated motor symptoms in susceptible patients.

Key words: Tau; Lithium; Parkinson's disease; Iron; Bipolar affective disorder, Neuroprotection, Neurodegeneration

Introduction

Lithium was identified as a psychoactive drug in the mid-20th century[1], and remains the primary therapy for bipolar affective disorder [2] (although it is often used in other psychiatric disorders also). Unfortunately it has a narrow therapeutic window limited by adverse effects[3, 4], and neither the mechanism of action nor its associated toxicity are well understood. Lithium modulates multiple key cellular signaling molecules[3, 5], including inositol monophosphatase (IMPase) and glycogen synthase kinase 3 (GSK-3), considered likely to be therapeutic targets[3]. Parkinson-like hand tremor is a common adverse effect of lithium therapy, and limited cross-sectional studies and several case reports have raised concern that lithium may increase the risk for extra-pyramidal syndromes (e.g. dyskinesia) in overdose, but possibly also at appropriate maintenance levels[6-15]. Recently, long-term lithium use was reported as associated with an increased incidence of antiparkinson drug use or a PD diagnosis[16]. Whether lithium could induce extra-pyramidal syndromes by neurotransmitter imbalance (like 1st generation antipsychotics such as haloperidol) or by damage to the basal ganglia is not known.

While a previous study demonstrated the neurotoxic potential of lithium in mice treated with a dose considered to be within the therapeutic range (2.55g/kg in food)[17], lithium has been more extensively investigated for a host of neuroprotective properties in various neurological and psychiatric models including cerebral ischemia/reperfusion injury[18] and other neurotoxic insults[19]. A recent study[19] of adolescents at ultra-high risk for psychosis[20] found that low dose lithium treatment over 4 months lowered hippocampal T_2 relaxation time (T_2*), which was taken to signify neurochemical improvements that could underlie potential neuroprotective benefits of low-dose lithium as an approach to prevent the onset of psychosis[21, 22]. However, a reduction of

T_2* can also be caused by an elevation of brain iron, and has been used to map such changes in diseases where iron levels rise, such as cortical tissue in Alzheimer's disease (AD)[23].

Lithium has attracted considerable interest as a therapeutic candidate in AD research. In neuronal cultures, lithium is reported to decrease tau phosphorylation[24-27] and to inhibit Aβ generation[28-30]. In Aβ-overexpressing transgenic models for AD, lithium treatment consistently decreases Aβ levels, GSK-3 activity and tau phosphorylation[29, 31-34]. In such models, lithium is reported to prevent Aβ toxicity[32], preserve dendritic structure[31], promote neurogenesis[34] and rescue Aβ-induced cognitive impairment[31, 33, 34]. Similarly, in transgenic mice that overexpress pathogenic mutant tau, lithium treatment reduced levels of hyperphosphorylation[35-39]. Despite these promising pre-clinical findings, lithium failed to show therapeutic efficacy for AD in a 10-week multicenter, randomized, single-blind, placebo-controlled trial, with no significant effects on CSF Aβ, CSF phospho-tau, or cognitive endpoints[40].

Nevertheless, lowering total tau expression is still being explored as a potential treatment for AD, and lithium is still being considered as a treatment option since it lowers both tau protein and mRNA levels in cultured cortical neurons[41, 42]. Supporting this concept, long-term (5 months) lithium treatment of PrP T44 tau transgenic mice resolved tau aggregates by promoting ubiquitination and degradation of tau, rather than altering GSK-3 activity[36].

We, and others, have reported concerns that lowering levels of brain tau could induce age-dependent neurodegeneration[43-45]. In tauopathies (such as AD and Parkinson's disease (PD)), insoluble tau aggregates are accompanied by a fall in soluble tau levels in affected tissue[43, 46-51]. We have argued that this will lead to a loss of tau function that could cause neurodegeneration, since tau functions to lower neuronal iron levels by promoting the presentation of the amyloid

protein precursor (APP) to the neuronal surface[43], where it promotes the efflux of iron[52-54]. Without soluble tau, neurons accumulate iron to toxic levels, and so, tau knockout mice develop a parkinsonism with impaired-cognition phenotype that is rescued by iron chelation[43, 44]. Iron accumulation in the substantia nigra (SN) is a robust feature of PD, and is a sufficient cause for parkinsonism (reviewed[55]). There has been one case report of such SN iron elevation with extrapyramidal signs following long-term lithium treatment[56]. We hypothesized that, since lithium lowers neuronal tau, lithium could engender SN iron accumulation and induce parkinsonian neurodegeneration, explaining a cryptogenic aspect of its adverse effects profile.

Materials and methods

Reagents. Reagents were purchased from Sigma, Australia, unless specified.

The lithium clinical imaging study. The lithium clinical imaging study has been previously described[19]. The pilot study was conducted as an open-label, non-randomised, controlled single center study. Participants were consecutive referrals to the Personal Assessment and Crisis Evaluation (PACE) Clinic, a specialist clinic for young people at ultrahigh risk (UHR) for psychosis[20]. PACE is a subprogram of ORYGEN Youth Health, a specialist service for young people with emerging mental disorders. Inclusion criteria for PACE were: (1) age between 14 and 30 inclusive, (2) resident of the Melbourne metropolitan area or the ability to travel to the PACE clinic at least once a week, and (3) meeting PACE UHR criteria. UHR criteria were determined using the Comprehensive Assessment of the At Risk Mental State (CAARMS)[57]. Rationale and validity for these criteria have been fully described elsewhere[58]. Exclusion criteria were: (1) medical or neurological conditions that may diminish functioning or that may account for some of the symptoms leading to the initial referral e.g. epilepsy, (2) clinically relevant

biochemical or hematological abnormalities, (3) serious coexisting illnesses such as liver or renal insufficiency, significant cardiac, vascular, pulmonary, gastrointestinal, endocrine, neurological or metabolic disturbances (including patients known to be HIV positive), (4) history of previous acute psychotic episodes either treated or untreated, (5) a current score of 5 or 6 on the CAARMS Mania item or a history of a previous manic episode, (6) any previous use of neuroleptic or mood stabilizing medications, (7) history of severe drug allergy or hypersensitivity, (8) history of intellectual disability (IQ < 70), (9) inability to understand or communicate in English. All UHR subjects received PACE treatment as usual throughout the course of the study including psychological and medical treatment. Use of antidepressants was allowed if UHR patients met criteria for major depression. UHR subjects in the low-dose lithium group took one slow-release 450 mg tablet of lithium carbonate each night for the entire study period (3 months), intended to achieve serum lithium levels of 0.3- 0.5 mM, in addition to treatment as usual.

Baseline MRI scans and clinical assessments were conducted prior to commencement of the low-dose lithium treatment, and within two weeks of admission to the study. Monitoring of psychopathology and tolerability measures occurred at monthly intervals, and follow-up scanning was conducted as close as possible to three months after baseline (median for the control group was 3.0 months, range 0.8-27 months; for the lithium group 3.8 months, range 1.6-5.9 months, some subjects in both groups not completing the full treatment period). Extrapyramidal side effects were not systematically assessed. The local research and ethics committee approved the study protocol. All participants gave written informed consent. Additional written informed consent was obtained from parents or guardians for participants

aged 14 - 18. Participants were made aware that they could withdraw from the study at any time and that withdrawal would not compromise access to any clinical services.

Brain imaging and SN T_2 relaxometry. All scans were performed on a 3T GE LX Horizon scanner (GE Healthcare, Milwaukee, USA) at the Brain Research Institute, Victoria, Australia. Eight tilted, coronal T_2-weighted images (perpendicular to the long axis of the hippocampus) were obtained over a range of echo times (29 to 231msec; TR=4sec, slice thickness= 6mm with 1.5mm gap, matrix 256x256, FOV 24cm). Single exponentials were then fitted to the image data of corresponding voxels from these eight echoes using iBrain (Brain Research Institute, Melbourne). This created a series of T_2 maps, one for each coronal slice. The brightness of each individual voxel on this map represents its calculated T_2 relaxation time. The images were then analyzed in various regions of interest with reference to a standard neuroanatomical atlas, by two raters who were blinded to treatment group, and quantified using ANALYZE 7.2 software (Mayo Clinic, Rochester, Minn), as described[19].

Primary neuron culture. Primary neurons were prepared as previously described[43]. Briefly, cortices of wild type and tau knockout embryos (day 14) were dissected and dissociated in 0.025% (w/v) trypsin. The neurons were plated (Nunc) at a density of 600,000 cells per cm^2 in plating medium (DMEM with 10% fetal calf serum, 5% house serum, and 10 mg L^{-1} gentamycin sulfate, Invitrogen). After 2 h incubation, the neurons were changed to Neurobasal supplemented medium (with B27, 500 μM glutaMAX and 10 μg mL^{-1} gentamycin sulfate). Experiments were performed 7 d later. Confluent cells were incubated in Neurobasal medium solution before treatment with various concentrations of lithium chloride for 18 hours with or without radioactive ^{59}Fe or ^{65}Zn, or various compounds (L690,330; 6-bromoindirubin-3'-oxime, BIO) at

concentrations indicated. The cells were then harvested, with half the batch lysed using lysis buffer (1% Triton-X100, 50mM Tris-HCl, 150mM NaCl, 1mM EDTA, pH7.4 together with 1:50 proteinase inhibitor and 1:1000 kinase inhibitor I&II), and the other half retained for metal analysis (see below), or assayed for radioactive tracers by γ-counter.

^{59}Fe-loaded transferrin and ^{65}Zn preparation. Purified human apo-transferrin (Tf) was loaded with ^{59}Fe (PerkinElmer), to form Tf(^{59}Fe)$_2$ as described [43, 52]. Neurons were incubated with 1.0 x 10^{-6} M Tf(^{59}Fe)$_2$ in serum-free Neurobasal supplemented medium for periods indicated. At the conclusions of the treatments, neurons were washed thoroughly with PBS, and harvested with trypsin. All media and cell lysates were measured by γ-counter (Wizard 3, Perkin Elmer) for counts/min (CPM). For iron efflux assay, cells were incubated at 37˚C and medium was removed at select time points. A comparable time course control study was performed at 4˚C to account for non-specific binding of ^{59}Fe to the membrane surface.

^{65}Zn experiments were adapted from a previous publication[59]. Briefly, serum-free Neurobasal supplemented medium was mixed with 0.04M Bq ^{65}Zn (Oak Ridge Laboratory) and unlabeled $ZnCl_2$ (20 μM). After 18 hours of treatment, the reaction was stopped by washing cell monolayers three times with ice-cold non-labeled HBSS (with 2 mM L-histidine and 5 mM EDTA). The cells were then harvested and measured for ^{65}Zn retention by γ-counter (1282 CompuGamma, LKB Wallac).

Mouse tissue preparation. All mice were housed in a conventional animal facility according to standard animal care protocols and fed standard laboratory chow (Meat Free Rat and Mouse Diet, Specialty Feeds, Australia) and tap water *ad libitum*. All animal procedures were approved

by the Florey Institute animal ethics committee (10-017) and were performed in accordance with the National Health and Medical Research Council guidelines. Tau knockout[60], APP knockout[52] and background C57Bl6/SV129 mice stocks raised under the same conditions, were maintained homozygously, with backcrossing to the parental inbred strain every 3 generations. The mouse was euthanized with an overdose of sodium pentobarbitone (Lethabarb, 100mg/kg) and perfused with ice-cold saline before tissues were collected. Body weight and total brain wet weight were recorded. Once extracted, the right brain hemisphere was micro-dissected and stored at -80°C until required. The left brain hemisphere was fixed in 4% paraformaldehyde for 24 h, and then transferred to 30% Sucrose + PBS (pH 7.4) and kept at 4°C overnight for tyrosine hydroxylase (TH) immunohistochemistry and brain section analysis.

Lithium treatment to mice. 3-month-old male Bl6/C57J mice (used in **Figure 2**) as well as age-matched tau knockout, APP knockout, and background control (BL6/129sv) mice (used in **Figure 4**) were randomly assigned (by Excel) and orally gavaged with lithium chloride (3.6mg/kg/day, freshly dissolved in 0.9% NaCl, 0.5% Na-carboxymethylcellulose, 0.5% benzyl alcohol, and 0.4% Tween-80, with the use of an oroesophageal needle, continuously for 21 days) or the solution alone. Behavioral tests were performed at Day18-21, 2 hours after the daily lithium dose. To control for effects of potential acute sedation, drug-naive Bl6/C57J mice were treated with a single dose of diazepam (3mg/kg) or lithium (3.6mg/kg) and the performance tests carried out 2 hours later.

Behavioral measurements: *Pole test* assessment was performed as previously described[43]. Briefly, mice were placed vertically on a 30 cm vertical, 1 cm diameter pole placed within in their home cage, where mice make an 180˚ turn and return to the base of the pole. On the day

prior to testing (day 1), the animals were habituated to the pole and allowed five consecutive trials. Animals were then recorded via digital video on the test day (day 2). The interval time for the mouse to turn toward the ground ('time to turn'), and to reach the ground ('time to finish') were both recorded. Each mouse underwent five trials and the average was used in analysis. When mice were unable to turn and move down the pole, the trial was determined as incomplete. *Rotarod assessment* was performed as previously described[43]. Briefly, mice were assessed using a Panlab Rotarod apparatus in an accelerating model with triplicate measurements (maximum time of 2.5 min; speed increases every 8s). The time on the rod as well as the final speed of the rod was recorded and the triplicates averaged for analysis. *Open field test.* Spontaneous motor activity of mice was measured using a photo-beam activity system (Truscan 2.0, Coulbourn Instruments) as previously described[43]. The test area was 25.4 cm wide by 25.4 cm deep by 40.6 cm high. The mouse was placed in the chamber for one hour to allow acclimatization to its surroundings. Parameters of movements were calculated from the interception of beams to provide an XY coordinate. For *Y maze test*, a Y-shaped grey-painted timber with arms 29.5 cm long × 7.5 cm wide × 15.5 cm high was used as previously described[43]. All mice were subjected to a 2-trial Y-maze test separated by a 1 h intertrial interval to assess spatial recognition memory, with all testing performed during the light phase of the circadian cycle. The 3 identical arms were randomly designated start arm, novel arm, and other arm. Visual cues were placed on the walls of the maze. The first trial (training) was for 10 min, and the mice were allowed to explore only 2 arms (starting arm and other arm). For the second trial (retention) mice were placed back in the maze in the same starting arm, and allowed to explore for 5 min with free access to all 3 arms. Behaviours were recorded on video during a 5 min trial and the Ethovision video-tracking system (Noldus, Netherlands) was used for analysis. Data are expressed as the percentage of

frequency and duration for novel arm entries made during the 5-min second trial. All behavioural tests were performed by an investigator blinded to the experimental group.

Anatomical morphology from brain slice. The anatomical morphology was examined as previously described[43]. Briefly, caudate/putamen (CPu) and cerebellum sections from mice were sectioned using a Leica Cryostat set at 50 μm thickness and areas of interest were measured using Image-J (v1.49b, NIH), using landmarks (anterior commissure for CPu, and flocculus for cerebellum) to identify the depth of coronal sectioning (bregma +0.26±0.01mm and bregma -6.12±0.01mm). Two sections per mouse per area were analysed. CPu area was defined by the boundaries of corpus callosum, lateral ventricle, and anterior commissure. Corpus callosum, neocortical and cerebellar cortical thicknesses were averaged from 5 measurements. All quantifications were blinded.

Tyrosine hydroxylase immunohistochemistry. Tyrosine hydroxylase (TH) immunohistochemistry was performed as previously described[43]. On a calibrated Leica Cryostat, 30 μm sections (1:3 series) were collected through the SN pars compacta (SNpc) (anteroposterior -2.92 to -3.64 mm from bregma, Mouse Atlas Figure 55 to Figure 61), generating 8 sections per mouse (the second of the three sections was analyzed). After a further brief fixation (4% paraformaldehyde for 30 seconds), sections were blocked in 3% normal goat serum (Millipore) and incubated with primary anti-TH rabbit polyclonal (1:3000, Millipore) overnight. The sections were then incubated with goat anti-rabbit secondary horse radish peroxidase-conjugated antibody for 3 hours (Millipore), followed by diaminobenzidine visualization (1% w/v in PBS + 1% w/v $CoCl_2$, 1% w/v $NiSO_4$) + 3% w/v hydrogen peroxide. TH immunostained sections were counter-stained

with Neutral Red to visualize the Nissl substance in all neurons before mounting on Superfrost-Plus slides.

Stereological estimation of nigra neurons. SN neuron number was estimated as previously described[43]. Briefly, both TH-positive and TH-negative, Nissl-positive neurons were scored according to the optical fractionator rules by an investigator blinded to the experimental group. Using an unbiased counting frame (x=35 μm, y = 45 μm) at regular intervals on a sampling grid (x=140 μm, y=140 μm), viewed through a 60 x 1.3 N.A. oil objective (DMLB Leica Microscope), cells were detected with a morphometry and design-based stereology software package (Stereo Investigator 10.04, Microbrightfield, Colchester, VT). The coefficients of error and coefficients of variance were calculated as estimates of precision and only values of <0.1 were accepted.

Dopamine and DOPAC measurement. Dopamine metabolites were measured as previously described[43]. Briefly, CPu tissues were homogenized in HPLC sample buffer (0.4M perchloric acid, 0.15% sodium metabisulfite and 0.05% EDTA) before centrifugation at 10,000 g at 4 ˚C for 10 minutes. Supernatants were used for dopamine measurement by a HPLC system (ESA Biosciences; model 584) coupled to an electrochemical detector (ESA Biosciences; Coulochem III detector) (E1:-150 mV, E2:+220 mV, and guard cell: +250 mV). 50 μL was injected onto a MD-150 reverse phase C18 column (ESA Biosciences) and elution was performed at a flow rate of 0.6 mL/min in the mobile phase (75 mM sodium dihydrogen phosphate, 1.7 mM 1-octanesulfonic acid sodium salt, 100 mL/L triethylamine, 25 mM EDTA, 10% acetonitrile, pH 3). Peaks were identified by retention times set to known standards. Data were normalized to wet weight tissue.

Metal Analysis. Metal content was measured as previously described[43]. Briefly, samples from each experimental condition were freeze-dried, and then re-suspended in 69% nitric acid (ultraclean grade, Aristar) overnight. The samples were then heated for 20 min at 90 ˚C, and an equivalent volume of hydrogen peroxide (30%, Merck) was added for a further 15 min incubation at 70 ˚C. The samples were diluted in double-distilled water and assayed by inductively coupled plasma mass spectrometer (Ultramass 700, Varian). Each sample was measured in triplicate and the concentrations determined from the standard curve were normalized to tissue wet weight.

Western Blot. Samples from each experiment were homogenized in PBS (pH=7.4) with EDTA-free protease inhibitor cocktail (1:50, Roche) + phosphatase inhibitors I and II (1:1000) and centrifuged at 100,000 g for 30 minutes. Protein concentration of the supernatant following centrifugation was determined by BCA protein assay (Pierce). Aliquots of soluble tissue fraction with equal protein concentrations were separated in 4-12% bis-Tris gels with NuPAGE MES running buffer (Invitrogen), and transferred to nitrocellulose membranes by iBlot (Invitrogen). The membranes were blocked with milk (10% w/v) and probed with appropriate primary and secondary IgG-HRP conjugated antibodies (Dako). Enhanced chemiluminescence detection system (GE Healthcare) with the Fujifilm LAS-3000 was used for visualization. Densitometric quantification of immunoreactive signals was performed by ImageJ (1.49b, NIH) and normalized to the relative amount of β-actin and expressed as a percentage of the mean of the control group. The following primary antibodies were used in the current study: anti-β-actin (Sigma), anti-tau (DAKO), anti-pTau396 (Invitrogen).

Statistics. Statistical analysis was carried out in Prism 6 (GraphPad Software Inc) and power calculations were performed using PASS 13 (trial version, NCSS Statistical Software, USA) based on the variance of results in our previous publication10 and in pilot experiments. Equivalence of variance between experimental groups was confirmed using a Levene's test, when applicable. Normal distribution was assumed for all statistical analyses. All tests were two-tailed, with the level of significance set at 0.05. Specific types of test used for each experiment are described in Figure legends.

Results

Low dose lithium treatment induces reversible T_2 changes in the substantia nigra consistent with iron elevation*

To determine whether lithium treatment has the potential to raise nigral iron levels, we analyzed this nucleus in scans from a previous clinical trial[19]. The impact of low dose lithium treatment on hippocampal tissue integrity in individuals at UHR for psychosis was assessed by T_2 relaxometry in an open-labeled, non-randomized, controlled, single center pilot study. Participants were treated with lithium or as usual for three months, and repeated 3T magnetic resonance images were taken from participants before commencement of the study (Scan one), and after drug withdrawal (Scan two). Lithium treatment induced a decrease in hippocampal T_2 relaxation time[19], which could indicate an improvement in various neuropathologies (e.g. edema) but could also reflect an increase in tissue iron[61-65].

Since iron elevation in the SN could contribute to Parkinson-like side effects such as the commonly observed hand tremor, we revisited this study and measured T_2 relaxation in this region, as well as other comparison regions in the same coronal planes (as marked in **Supplementary Figure 1a**, with reference to a standard neuroanatomical atlas). We found that the average T_2 relaxation time in the SN of the lithium group at three months (Scan two) was significantly reduced from baseline (Scan one) (-5%, $p = 0.007$), and significantly lower than the control (treatment as usual) group at the same time point (-7%, $p < 0.001$; **Figure 1a-b**), consistent with iron accumulation or edema. The pattern of changes was similar in both hemispheres. Other regions analyzed, caudate and lenticular nucleus (LN), showed no change in T_2 relaxation time ($p = 0.18$ for caudate; $p = 0.29$ for LN; **Supplementary Figure 1b**) compared

to the baseline scan. The lateral ventricular cross-sectional area (LV) was also unchanged from baseline (p = 0.177; **Supplementary Figure 1b**).

Iron accumulation and parkinsonism in a mouse model of lithium therapy

To test whether lithium-induced relaxometry changes could be due to brain iron accumulation, 3-month old C57/Bl6J mice were orally administered lithium chloride at a low therapeutic dose[40] (3.6mg/kg body weight/day) for 21 days. The dose was well-tolerated and body weight was unaltered during the treatment period (p = 0.188; **Figure 2a**). Lithium levels were elevated in all tested tissues (p<0.001 for cortex, SN, cerebellum, and liver), with the greatest proportional elevation in cortex (+263%) and SN (+152%; **Figure 2b**). Iron levels were increased in cortex (+40%, p=0.008) and SN (+19%, p=0.039), but not cerebellum, liver or plasma (**Figure 2c**). The effect of lithium on biological metals was specific to iron, with copper and zinc unaltered in all tested tissues (**Supplementary Figure 2a-b**). Lithium levels significantly correlated with iron levels in SN (p = 0.007, R^2= 0.62; **Figure 2d**) and cortex (p = 0.026, R^2= 0.439; **Supplementary Figure 3a**) in lithium-treated mice, consistent with elevated lithium causing an elevation in iron. The correlation was seen neither in sham-treated SN (R^2= 0.02; **Figure 2d**) nor cortex (R^2= 0.03; **Supplementary Figure 3a**), nor observed in the cerebellum of lithium- (R^2= 0.01) or sham-treated (R^2= 0.05) animals, a region that did not accumulate iron with lithium treatment (**Supplementary Figure 3b**). Neither copper nor zinc correlated with lithium in these tissues (**Supplementary Figure 3c-d**).

We assessed the brains of lithium-treated mice to determine whether a drop in soluble tau could explain the iron elevation[43]. As expected[36, 38, 39, 66], the fraction of brain tau phosphorylated at Ser396 was suppressed by lithium treatment (cortex: -40%, p = 0.034; SN: -43%, p = 0.039;

Supplementary Figure 4). We also discovered that lithium administration lowered PBS-soluble total tau levels in cortex and SN (cortex: -31%, $p = 0.032$; SN: -42%, $p < 0.001$; **Figure 2e**).

Since tau loss causes iron-mediated neurodegeneration with parkinsonism[43-45], we investigated whether the lithium treatment impaired motor function in these mice. Lithium-treated mice compared to sham-treated mice exhibited a significant increase in time to turn ($p = 0.008$; **Figure 2f**) and to finish ($p = 0.041$; **Supplementary Figure 5a**) on the Pole test, and significantly impaired performance on the accelerated Rotarod test as evidenced by reduced latency to fall ($p = 0.004$; **Figure 2g**), and lower average speed to fall (at speed 6, $p<0.001$; at speed 7, $p=0.015$; **Supplementary Figure 5b**). Rotarod impairment has previously been noted in 10 month old mice treated for 4 weeks with lithium, but the cause was not ascertained[39]. Lithium-treated mice also exhibited reduced locomotion distance ($p = 0.022$; **Supplementary Figure 5c**), reduced velocity ($p = 0.023$; **Supplementary Figure 5d**), and reduced average distance per movement ($p = 0.018$; **Supplementary Figure 5e**), without alterations in movement duration or time spent in the corners (data not shown) in the Open field test.

Control studies were performed to ascertain whether short-term sedation[4, 67] could have contributed to the motor impairment induced by lithium. Diazepam, a sedative with well-characterized effects on motor behaviors[68-71], was compared to lithium within 2 hours after dose for acute motor behavioral effects. Single-dose lithium or diazepam did not impair mouse Rotarod performance at this interval (**Supplementary Figure 6a**). Diazepam, but not lithium, induced a sudden drop in spontaneous locomotion 20 mins after dosing in the Open field test ($p = 0.006$; **Supplementary Figure 6b)**. These data indicate that the motor impairments induced by lithium were not due to sedation.

To determine whether the motor deficits induced by lithium could be due to Parkinson-like neuropathology, the TH-immunoreactive (dopaminergic) neurons within the SN were stereologically counted. The dopaminergic neurons were significantly decreased in mice treated with lithium for 21 days (-30%, $p < 0.001$; **Figure 2h-i**), but TH-negative, Neutral Red-positive neurons were unaltered (**Supplementary Figure 7a**). Accompanying this loss, dopamine (-40%, $p = 0.023$; **Figure 2j**) and DOPAC (-37%, $p = 0.024$; **Supplementary Figure 7b**) levels in the striatum were also decreased in lithium-treated mice. Excess dopamine induces hyperactivity, a characteristic of mania[72], and is attenuated by lithium treatment[73]. Lithium decreases dopaminergic release[74] and suppresses levels of dopamine and its metabolites in the striatal projection field and nucleus accumbens[75]. Our findings indicate that suppression of the SN-striatal dopaminergic pathway may contribute both to the motor deficits induced by lithium, as well as, potentially, to its long-term anti-manic and anti-psychosis properties.

Lithium induces tau-mediated iron accumulation in neuronal culture

Having found that by inducing nigral tau suppression lithium treatment of normal mice recapitulated a series of abnormalities that appear in tau knockout mice (nigral iron elevation with dopaminergic neurodegeneration and parkinsonism), we investigated the mechanism in mouse primary cortical neuronal cultures. Lithium (at non-toxic concentrations[29]) induced significant iron accumulation within 18 hours in a dose-dependent manner (5mM Li: +48%, $p = 0.005$; 10mM Li: +56%, $p < 0.001$; **Figure 3a**), but did not alter copper or zinc levels (**Figure 3b**), consistent with the changes in brain levels of these metals in mice treated with lithium (**Figure 2c**). Lithium (10 mM) significantly inhibited the efflux of iron (chased after ^{59}Fe loading) into the media ($p < 0.001$; **Figure 3c**), explaining the retention of iron. As expected,

lithium treatment (10 mM) had no effect on zinc retention in primary neurons treated with radio-labeled ^{65}Zn ($p = 0.176$, **Supplementary Figure 8**).

The activities of both inositol monophosphatase (IMPase) and GSK-3[5] are considered molecular targets for lithium's therapeutic effect in bipolar disorder[3]. L-690,330, a potent and more specific inhibitor of IMPase[76], had no effect on cellular iron level during the 18 hour incubation ($p = 0.106$; **Supplementary Figure 9a**), thus eliminating IMPase in the mechanism of iron accumulation induced by lithium. However, 6-bromoindirubin-3'-oxime (BIO), a potent and specific inhibitor of GSK-3[77], caused iron retention similar to the effect of lithium (+59%, p=0.002, **Supplementary Figure 9b**).

Both lithium and BIO are reported to decrease total tau protein levels in addition to their inhibitory effects of GSK in cultured neurons[42]. In agreement with previous reports[41, 42], we found that lithium (≥5 mM, 18 hours) suppresses tau protein levels in primary neurons (5mM Li: -48%, $p = 0.007$; 10mM Li: -35%, $p = 0.034$; **Figure 3d**) and in SH-SY5Y cells (5mM Li: -25%, $p = 0.003$; 10mM Li: -25%, $p = 0.002$; **Supplementary Figure 10a-b**). BIO (18 hours) also suppressed tau protein levels in primary neuronal culture (1μM BIO: -25%, $p = 0.043$; 2μM BIO: -26%, $p = 0.048$; **Supplementary Figure 10c-d**), which may be the mechanism for its ability to increase neuronal iron levels.

To demonstrate the requirement for tau in the mechanism of lithium-induced iron accumulation in neurons, lithium (10 mM, 18 hours) was administered to tau knockout primary neurons and compared with background-matched wild type neurons (**Figure 3e**). As previously shown[43], tau KO neurons retained more iron (+20%, $p = 0.032$) compared to wild type neurons. As expected, lithium treatment (10 mM, 18 hours) of wild type neurons induced a significant

accumulation of iron (+20%, $p = 0.038$), but lithium treatment of tau knockout neurons induced no further iron accumulation. Thus, lithium-induced neuronal iron accumulation requires the expression of tau protein.

Tau knockout and APP knockout mice are resistant to neurodegeneration caused by chronic lithium administration

Tau mediates neuronal iron efflux by facilitating the trafficking of APP to the cell surface, where it stabilizes the iron export channel ferroportin[43, 52-54]. To test whether lithium-induced iron accumulation requires APP, we applied the same lithium treatment to tau knockout mice, APP knockout mice, and their background-matched wild type mice. We studied mice at 3-months of age, because the knockouts have yet to develop the age-dependent elevation in brain iron levels[43, 44].

All three strains showed no weight reduction during 21 days of lithium treatment (**Figure 4a**) even though APP knockout were lighter in weight (as reported previously[78]). Lithium treatment predictably caused an elevation in mouse plasma lithium levels (WT: +6.6 fold, $p < 0.001$; tau KO: +6.7 fold, $p < 0.001$; APP KO: +4.3 fold, $p = 0.007$; **Figure 4b**), although the levels in all three strains remained well below the lower limit of the therapeutic concentration range[40]. As with the Bl6/C57J mice (**Figure 2c**), lithium treatment induced iron elevation in both the cortex and SN of the littermate Bl6/129Sv mice (cortex: +15%, $p = 0.031$; SN: +20%, $p = 0.041$), but despite lithium elevations in brain regions being commensurate to those in Bl6/C57J mice (**Figure 2b**), tau- and APP- knockout mice were unaffected (**Figure 4c-d**), consistent with the neuronal culture findings (**Figure 3e**). Brain copper or zinc levels were again unaffected

(**Supplementary Figure 11a-d**), and iron levels in the cerebellum and liver were unaltered (**Supplementary Figure 11e-f**), by lithium treatment in all three strains.

Ablation of APP abolished lithium-induced iron accumulation (**Figure 4c-d**), despite soluble tau protein levels in cortex and SN of APP knockout mice treated with lithium being suppressed comparably to wild type (cortex: -19%, $p = 0.041$ for wild type and -41%, $p = 0.006$ for APP KO; SN: -42%, $p < 0.001$ for wild type and 21%, $p = 0.041$ for APP KO; **Figure 4e, Figure 4f, Supplementary Figure 12**). These results confirm our prediction that lithium-induced brain iron accumulation requires both tau and APP expression, with tau being upstream in the APP-associated iron homeostatic pathway.

As lithium-induced Parkinson-like symptoms such as hand tremor may be mediated by iron accumulation in the brain, disabling lithium-induced SN iron accumulation in tau and APP knockout mice (**Figure 4d**) should also prevent motor deficits and SN neuronal loss. Indeed, lithium-induced motor deficits were abolished in tau and APP knockout mice, as evidenced by unaffected time to turn (WT, $p = 0.020$; **Figure 4g**) and time to finish (WT, $p = 0.048$; **Supplementary Figure 13a**) in the Pole test, and unaltered average distance per movement (WT, $p = 0.049$; **Figure 4h**), distance of locomotion (WT, $p = 0.020$; **Supplementary Figure 13b**), and velocity (WT, $p = 0.048$; **Supplementary Figure 13c**) in the Open field test. Untreated APP knockout mice did show baseline motor deficits (**Figure 4g-h, Supplementary Figure 13a-c**), as previously reported[78], but these were not worsened by lithium. Tau or APP ablation also negated SN dopaminergic neuron loss induced by lithium treatment (WT, $p < 0.001$; **Figure 4i, Supplementary Figure 14a**). Together, these results support the conclusion that lithium-induced parkinsonism is mediated by iron accumulation, which is tau- and APP-dependent.

Since lithium treatment also increases cortical iron levels (**Figures 2c & 4c**), we investigated its effect on cognitive performance and related brain anatomy. In the Y-maze test, we found the memory performance of wild type mice was markedly impaired by 21 days of lithium treatment ($p = 0.022$), but, as with the Pole test (**Figure 4g**), tau- and APP- KO mice were unaffected by lithium (**Figure 4j**). Accordingly, lithium treatment caused brain atrophy in wild type mice, evidenced by enlarged lateral ventricular area (+72%, $p = 0.023$; **Figure 4k,l**), shrinkage of CPu area (-13%, $p = 0.011$; **Supplementary Figure 14b**), and reduced cortical thickness (-7%, $p = 0.040$; **Supplementary Figure 14c**), without affecting corpus callosum width (**Supplementary Figure 14d**). Again, lithium did not induce brain atrophy in tau- or APP- KO mice (**Figure 4l, Supplementary Figure 14c,d)**. These toxic consequences of lithium administration to cortical thickness are in agreement with a previous report that found cortical neuronal apoptosis in mice upon chronic lithium treatment[17].

Discussion

Lithium has an established record of efficacy in bipolar affective disorder, despite a narrow therapeutic window limited by various toxicities of uncertain mechanism. Here we found that lithium may contribute to nigral and cortical degeneration, with motor and cognitive impairment in wild-type mice, recapitulating the neurophysiological and neurochemical phenotypes of aged tau knockout mice[43, 44]. Lithium suppresses tau protein levels in cultured neurons and in mice, causing iron accumulation through a tau- and APP-dependent interaction. The T_2 relaxation time changes in the human lithium trial are consistent with iron elevation in hippocampus and SN. Although homeostasis keeps brain iron levels stringently stable in health, and geared to resist depletion[79], rodent studies have shown that nearly 10% of brain iron is in relatively rapid exchange with dietary iron[52, 80], indicating that in order to prevent iron accumulation, iron efflux

from the brain must be constantly active. It is this mechanism that lithium inhibits, by, at least in part, suppressing tau expression. Tau knockout mice develop iron-induced neurodegenerative changes at 12 months of age [43, 44] but lithium-induced toxic iron accumulation occurs within weeks. This is probably because the tau knockout mice in youth have the benefit of upregulated compensatory responses from other microtubule associated proteins [45] in contrast to the more acute suppression of tau expression by lithium treatment. Our findings add to the evidence that lithium at therapeutic (and eventually even at subtherapeutic) chronic doses can cause neurodegeneration[17], and provide a possible mechanism for adverse neurological effects in susceptible individuals.

Parkinsonism is an uncommon adverse effect of lithium treatment, but hand tremor is common and may be age- and dose- dependent [81-83]. In addition, lithium use was found to be associated with an increased incidence of antiparkinson drug use or a PD diagnosis[16]. The mechanisms underlying these motor abnormalities are not known, but could be due to persistent or transient extrapyramidal syndromes caused by damage to the basal ganglia and SN. Iron may play a critical role in promoting SN pathology in PD[55, 84], and our findings demonstrate how lithium could worsen iron-mediated SN damage. SN iron accumulation in trial subjects may have occurred after only 3 months of low-dose lithium treatment (**Figure 1b**), although no conspicuous motor abnormalities were reported in this group. Additionally, our findings in mice support the possibility that lithium-induced parkinsonism can become irreversible in a proportion of patients[6-8, 11, 15].

Unexpectedly, we found that lithium treatment at doses inducing blood levels well below the human therapeutic range caused cognitive impairment and brain atrophy in mice after 3 weeks (**Figure 4j-l**). It has been shown previously that lithium treatment at therapeutic doses can cause

cortical neuronal apoptosis[17], which may explain our findings. While lithium treatment was previously reported to correct the smaller hippocampal volumes in patients with bipolar disorder[85], there is also evidence that long-term lithium treatment is associated with cognitive impairment[86-89] and brain atrophy[89]. Neurodegeneration in mice administered lithium to achieve blood levels that are easily tolerated by humans may reflect different pharmacodynamics in the species, or that humans are less sensitive than mice to lithium-induced neurotoxicity.

Lithium-induced motor deficits in mice are reported to involve the calcineurin/nuclear factor of activated T cells (NFAT)/Fas ligand signaling pathway, and prevented by inhibition of calcineurin, or knockout of Fas[17]. Iron modulates calcineurin activity[90, 91], and can thereby impact the NFAT/Fas signaling pathway. Treatment with iron dramatically elevates NFAT activity[92, 93] while administering the iron chelator deferoxamine abolishes iron-induced NFAT activation[92, 93]. Together with our current data, a proposed model pathway emerges (**Figure 5**) where lithium suppresses tau protein levels, thus preventing APP trafficking to the cell surface and resulting in neuronal iron retention. In turn, this activates calcineurin/NFAT/Fas signaling, induces cortical and nigral neuronal apoptosis and engenders motor and cognitive disability.

Lithium was an attractive drug candidate for AD since its target, GSK-3, regulates both Aβ production and tau phosphorylation[5]. However, it is neither a potent nor specific inhibitor of GSK-3[94]. In fact, neuronal deficits have been reported to result from both genetic reduction and specific inhibition of GSK-3[95, 96], highlighting the risk of inhibiting this enzyme[97]. Lithium arrests neuropathology in some AD rodent models[36, 38, 39], but these are aggressive models driven by transgene overexpression, where the benefits of lithium inhibiting a dominant pathological target (e.g. tau hyperphosphorylation) outweigh lithium-induced neurotoxicity. The lithium-

induced neurotoxicity that we, and others[17, 39], observed might only be detected in normal mice or mice that do not express a neuropathology that is inhibited by lithium.

Our current study might help explain the failure of trials of lithium for AD[40, 98] and ALS[99-101], both diseases where elevated iron in the affected tissue has been implicated in pathogenesis[52, 102-104]. Despite the neurotoxicity in mice that our studies have elaborated, clinical lithium pharmacotherapy has predominantly neurotrophic benefits in the treatment of bipolar disorder. It is an intriguing hypothesis to consider that these benefits might be related to the correction of iron deficiency in certain brain regions.

Competing Interests

Dr Finkelstein is a paid scientific consultant for Prana Biotechnology Ltd. Dr. Bush is a shareholder in Prana Biotechnology Ltd., Eucalyptus Pty Ltd., Mesoblast Pty Ltd., Brighton Biotech Inc, Nextvet Ltd, and a paid consultant for Collaborative Medicinal Developments Pty Ltd. C. Pantelis has participated on Advisory Boards for Janssen-Cilag, Astra-Zeneca, Lundbeck, and Servier. He has received honoraria for talks presented at educational meetings organised by Astra-Zeneca, Janssen-Cilag, Eli-Lilly, Pfizer, Lundbeck and Shire.

Authors' Contributions

P.L. and A.I.B. conceived and raised funds for the study. P.L., S.A., J.D., R.C., D.I.F., and A.I.B. designed and performed the experiments. A.T.A., S.M., I.V., M. G. and Q.Z. assisted with the experiments. S.J.W., G.B., C.P., P.M. A.R.Y. conducted the lithium human trial. P.L. and A.I.B integrated the data and wrote the drafts of the manuscript. All authors edited the manuscript.

Acknowledgments

The authors thank A. Sedjahtera, L. Lam, L. Gunawan, L. Bray, and K. Wikhe for technical assistance. The authors also acknowledge L. Phillips and B. Nelson for their contributions in lithium human trial. Supported by funds from the Australian Research Council, the National Health & Medical Research Council (NHMRC) of Australia, the Cooperative Research Center for Mental Health, Alzheimer's Australia Dementia Research Foundation, and National Natural Science Foundation of China (81571236). A. Bush was supported by a NHMRC Australia Fellowship (AF79) and a NHMRC Senior Principal Research Fellowship (1103703). C. Pantelis was supported by a NHMRC Senior Principal Research Fellowship (628386 & 1105825). The imaging work on lithium was supported by NHMRC Project grant (145627) and NHMRC Program grants (350241, 566529). Florey Institute of Neuroscience and Mental Health acknowledges the strong support from the Victorian Government and in particular the funding from the Operational Infrastructure Support Grant.

Supplementary information is available at *Molecular Psychiatry*'s website.

References

1. Cade JF. Lithium salts in the treatment of psychotic excitement. *The Medical journal of Australia* 1949; **2**(10)**:** 349-352.

2. Geddes JR, Goodwin GM, Rendell J, Azorin JM, Cipriani A, Ostacher MJ *et al.* Lithium plus valproate combination therapy versus monotherapy for relapse prevention in bipolar I disorder (BALANCE): a randomised open-label trial. *Lancet* 2010; **375**(9712)**:** 385-395.

3. Phiel CJ, Klein PS. Molecular targets of lithium action. *Annual review of pharmacology and toxicology* 2001; **41:** 789-813.

4. Grof P, Müller-Oerlinghausen B. A critical appraisal of lithium's efficacy and effectiveness: the last 60 years. *Bipolar Disord* 2009; **11 Suppl 2:** 10-19.

5. Lei P, Ayton S, Bush AI, Adlard PA. GSK-3 in Neurodegenerative Diseases. *Int J Alzheimers Dis* 2011; **2011:** 189246.

6. Ghadirian AM, Annable L, Bélanger MC, Chouinard G. A cross-sectional study of parkinsonism and tardive dyskinesia in lithium-treated affective disordered patients. *The Journal of clinical psychiatry* 1996; **57**(1)**:** 22-28.

7. Dallocchio C, Mazzarello P. A case of Parkinsonism due to lithium intoxication: treatment with Pramipexole. *J Clin Neurosci* 2002; **9**(3)**:** 310-311.

8. Shopsin B, Gershon S. Cogwheel rigidity related to lithium maintenance. *The American journal of psychiatry* 1975; **132**(5)**:** 536-538.

9. Reches A, Tietler J, Lavy S. Parkinsonism due to lithium carbonate poisoning. *Archives of neurology* 1981; **38**(7)**:** 471.

10. Apte SN, Langston JW. Permanent neurological deficits due to lithium toxicity. *Annals of neurology* 1983; **13**(4)**:** 453-455.

11. Lang AE. Lithium and parkinsonism. *Annals of neurology* 1984; **15**(2)**:** 214.

12. Muthane UB, Prasad BN, Vasanth A, Satishchandra P. Tardive Parkinsonism, orofacial dyskinesia and akathisia following brief exposure to lithium carbonate. *J Neurol Sci* 2000; **176**(1)**:** 78-79.

13. Mazzini L, Oggioni GD, Nasuelli N, Servo S, Testa L, Monaco F. Disabling Parkinsonism following brief exposure to lithium carbonate in amyotrophic lateral sclerosis. *Journal of neurology* 2011; **258**(2)**:** 333-334.

14. Fallgatter AJ, Strik WK. [Reversible neuropsychiatric side effects of lithium with normal serum levels. A case report]. *Nervenarzt* 1997; **68**(7)**:** 586-590.

15. Perenyi A, Rihmer Z, Banki CM. Parkinsonian symptoms with lithium, lithium-neuroleptic, and lithium-antidepressant treatment. *Journal of affective disorders* 1983; **5**(2)**:** 171-177.

16. Marras C, Herrmann N, Fischer HD, Fung K, Gruneir A, Rochon PA *et al.* Lithium Use in Older Adults is Associated with Increased Prescribing of Parkinson Medications. *The American journal of geriatric psychiatry : official journal of the American Association for Geriatric Psychiatry* 2016; **24**(4)**:** 301-309.

17. Gómez-Sintes R, Lucas JJ. NFAT/Fas signaling mediates the neuronal apoptosis and motor side effects of GSK-3 inhibition in a mouse model of lithium therapy. *J Clin Invest* 2010; **120**(7)**:** 2432-2445.

18. Taliyan R, Ramagiri S. Delayed neuroprotection against cerebral ischemia reperfusion injury: putative role of BDNF and GSK-3beta. *J Recept Signal Transduct Res* 2015**:** 1-9.

19. Berger GE, Wood SJ, Ross M, Hamer CA, Wellard RM, Pell G *et al.* Neuroprotective Effects of Low-dose Lithium in Individuals at Ultra-high Risk for Psychosis. A Longitudinal MRI/MRS Study. *Curr Pharm Des* 2012; **18**(4)**:** 570-575.

20. Yung AR, Phillips LJ, Yuen HP, McGorry PD. Risk factors for psychosis in an ultra high-risk group: psychopathology and clinical features. *Schizophr Res* 2004; **67**(2-3)**:** 131-142.

21. Benarous X, Consoli A, Milhiet V, Cohen D. Early interventions for youths at high risk for bipolar disorder: a developmental approach. *Eur Child Adolesc Psychiatry* 2016; **25**(3)**:** 217-233.

22. Berger GE, Wood S, McGorry PD. Incipient neurovulnerability and neuroprotection in early psychosis. *Psychopharmacology bulletin* 2003; **37**(2)**:** 79-101.

23. van Rooden S, Versluis MJ, Liem MK, Milles J, Maier AB, Oleksik AM *et al.* Cortical phase changes in Alzheimer's disease at 7T MRI: a novel imaging marker. *Alzheimer's & dementia : the journal of the Alzheimer's Association* 2014; **10**(1)**:** e19-26.

24. Hong M, Chen DC, Klein PS, Lee VM. Lithium reduces tau phosphorylation by inhibition of glycogen synthase kinase-3. *J Biol Chem* 1997; **272**(40)**:** 25326-25332.

25. Munoz-Montano JR, Moreno FJ, Avila J, Diaz-Nido J. Lithium inhibits Alzheimer's disease-like tau protein phosphorylation in neurons. *FEBS Lett* 1997; **411**(2-3)**:** 183-188.

26. Lovestone S, Davis DR, Webster MT, Kaech S, Brion J-P, Matus A *et al.* Lithium reduces tau phosphorylation: effects in living cells and in neurons at therapeutic concentrations. *Biol Psychiatry* 1999; **45**(8)**:** 995-1003.

27. Takahashi M, Yasutake K, Tomizawa K. Lithium inhibits neurite growth and tau protein kinase I/glycogen synthase kinase-3beta-dependent phosphorylation of juvenile tau in cultured hippocampal neurons. *J Neurochem* 1999; **73**(5)**:** 2073-2083.

28. Sun X, Sato S, Murayama O, Murayama M, Park JM, Yamaguchi H *et al.* Lithium inhibits amyloid secretion in COS7 cells transfected with amyloid precursor protein C100. *Neurosci Lett* 2002; **321**(1-2)**:** 61-64.

29. Phiel CJ, Wilson CA, Lee VM-Y, Klein PS. GSK-3alpha regulates production of Alzheimer's disease amyloid-beta peptides. *Nature* 2003; **423**(6938)**:** 435-439.

30. Su Y, Ryder J, Li B, Wu X, Fox N, Solenberg P *et al.* Lithium, a common drug for bipolar disorder treatment, regulates amyloid-beta precursor protein processing. *Biochemistry* 2004; **43**(22)**:** 6899-6908.

31. Rockenstein E, Torrance M, Adame A, Mante M, Bar-on P, Rose JB *et al.* Neuroprotective effects of regulators of the glycogen synthase kinase-3beta signaling pathway in a transgenic model of Alzheimer's disease are associated with reduced amyloid precursor protein phosphorylation. *J Neurosci* 2007; **27**(8)**:** 1981-1991.

32. Sofola O, Kerr F, Rogers I, Killick R, Augustin H, Gandy C *et al.* Inhibition of GSK-3 ameliorates Abeta pathology in an adult-onset Drosophila model of Alzheimer's disease. *PLoS Genet* 2010; **6**(9).

33. Toledo EM, Inestrosa NC. Activation of Wnt signaling by lithium and rosiglitazone reduced spatial memory impairment and neurodegeneration in brains of an APPswe/PSEN1DeltaE9 mouse model of Alzheimer's disease. *Mol Psychiatry* 2010; **15**(3)**:** 272-285, 228.

34. Fiorentini A, Rosi MC, Grossi C, Luccarini I, Casamenti F. Lithium Improves Hippocampal Neurogenesis, Neuropathology and Cognitive Functions in APP Mutant Mice. *PLoS ONE* 2010; **5**(12)**:** e14382.

35. Pérez M, Hernández F, Lim F, Díaz-Nido J, Avila J. Chronic lithium treatment decreases mutant tau protein aggregation in a transgenic mouse model. *J Alzheimers Dis* 2003; **5**(4)**:** 301-308.

36. Nakashima H, Ishihara T, Suguimoto P, Yokota O, Oshima E, Kugo A *et al.* Chronic lithium treatment decreases tau lesions by promoting ubiquitination in a mouse model of tauopathies. *Acta neuropathologica* 2005; **110**(6)**:** 547-556.

37. Noble WJ, Planel E, Zehr C, Olm V, Meyerson J, Suleman F *et al.* Inhibition of glycogen synthase kinase-3 by lithium correlates with reduced tauopathy and degeneration in vivo. *Proc Natl Acad Sci USA* 2005; **102**(19)**:** 6990-6995.

38. Engel T, Goñi-Oliver P, Lucas JJ, Avila J, Hernández F. Chronic lithium administration to FTDP-17 tau and GSK-3beta overexpressing mice prevents tau hyperphosphorylation and neurofibrillary tangle formation, but pre-formed neurofibrillary tangles do not revert. *J Neurochem* 2006; **99**(6)**:** 1445-1455.

39. Leroy K, Ando K, Héraud C, Yilmaz Z, Authelet M, Boeynaems J-M *et al.* Lithium Treatment Arrests the Development of Neurofibrillary Tangles in Mutant Tau Transgenic Mice with Advanced Neurofibrillary Pathology. *J Alzheimers Dis* 2010; **19:** 705-719.

40. Hampel H, Ewers M, Bürger K, Annas P, Mörtberg A, Bogstedt A *et al.* Lithium trial in Alzheimer's disease: a randomized, single-blind, placebo-controlled, multicenter 10-week study. *The Journal of clinical psychiatry* 2009; **70**(6)**:** 922-931.

41. Rametti A, Esclaire F, Yardin C, Cogné N, Terro F. Lithium down-regulates tau in cultured cortical neurons: a possible mechanism of neuroprotection. *Neurosci Lett* 2008; **434**(1)**:** 93-98.

42. Martin L, Magnaudeix A, Esclaire F, Yardin C, Terro F. Inhibition of glycogen synthase kinase-3beta downregulates total tau proteins in cultured neurons and its reversal by the blockade of protein phosphatase-2A. *Brain Res* 2009; **1252:** 66-75.

43. Lei P, Ayton S, Finkelstein DI, Spoerri L, Ciccotosto GD, Wright DK *et al.* Tau deficiency induces parkinsonism with dementia by impairing APP-mediated iron export. *Nat Med* 2012; **18**(2)**:** 291-295.

44. Lei P, Ayton S, Moon S, Zhang Q, Volitakis I, Finkelstein DI *et al.* Motor and cognitive deficits in aged tau knockout mice in two background strains. *Mol Neurodegener* 2014; **9**(1)**:** 29.

45. Ma QL, Zuo X, Yang F, Ubeda OJ, Gant DJ, Alaverdyan M *et al.* Loss of MAP function leads to hippocampal synapse loss and deficits in the Morris Water Maze with aging. *J Neurosci* 2014; **34**(21)**:** 7124-7136.

46. Zhukareva V, Vogelsberg-Ragaglia V, Van Deerlin VM, Bruce J, Shuck T, Grossman M *et al.* Loss of brain tau defines novel sporadic and familial tauopathies with frontotemporal dementia. *Ann Neurol* 2001; **49**(2)**:** 165-175.

47. Zhukareva V, Sundarraj S, Mann D, Sjogren M, Blenow K, Clark CM *et al.* Selective reduction of soluble tau proteins in sporadic and familial frontotemporal dementias: an international follow-up study. *Acta neuropathologica* 2003; **105**(5)**:** 469-476.

48. Ksiezak-Reding H, Binder LI, Yen S-HC. Immunochemical and biochemical characterization of tau proteins in normal and Alzheimer's disease brains with Alz 50 and Tau-1. *J Biol Chem* 1988; **263**(17)**:** 7948-7953.

49. Shin RW, Iwaki T, Kitamoto T, Sato Y, Tateishi J. Massive accumulation of modified tau and severe depletion of normal tau characterize the cerebral cortex and white matter of Alzheimer's disease. Demonstration using the hydrated autoclaving method. *Am J Pathol* 1992; **140**(4)**:** 937-945.

50. Khatoon S, Grundke-Iqbal I, Iqbal K. Levels of normal and abnormally phosphorylated tau in different cellular and regional compartments of Alzheimer disease and control brains. *FEBS Lett* 1994; **351**(1)**:** 80-84.

51. van Eersel J, Bi M, Ke YD, Hodges JR, Xuereb JH, Gregory GC *et al.* Phosphorylation of soluble tau differs in Pick's disease and Alzheimer's disease brains. *J Neural Transm* 2009; **116**(10)**:** 1243-1251.

52. Duce JA, Tsatsanis A, Cater MA, James SA, Robb E, Wikhe K *et al.* Iron-export ferroxidase activity of β-amyloid precursor protein is inhibited by zinc in Alzheimer's disease. *Cell* 2010; **142**(6)**:** 857-867.

53. McCarthy RC, Park YH, Kosman DJ. sAPP modulates iron efflux from brain microvascular endothelial cells by stabilizing the ferrous iron exporter ferroportin. *EMBO Rep* 2014; **15**(7)**:** 809-815.

54. Wong BX, Tsatsanis A, Lim LQ, Adlard PA, Bush AI, Duce JA. beta-Amyloid precursor protein does not possess ferroxidase activity but does stabilize the cell surface ferrous iron exporter ferroportin. *PLoS ONE* 2014; **9**(12)**:** e114174.

55. Ayton S, Lei P. Nigral iron elevation is an invariable feature of Parkinson's disease and is a sufficient cause of neurodegeneration. *BioMed research international* 2014; **2014:** 581256.

56. Campbell WG, Raskind MA, Gordon T, Shaw CM. Iron pigment in the brain of a man with tardive dyskinesia. *The American journal of psychiatry* 1985; **142**(3)**:** 364-365.

57. Yung AR, Yuen HP, McGorry PD, Phillips LJ, Kelly D, Dell'Olio M *et al.* Mapping the onset of psychosis: the Comprehensive Assessment of At-Risk Mental States. *Aust N Z J Psychiatry* 2005; **39**(11-12)**:** 964-971.

58. Yung AR, Phillips LJ, Yuen HP, Francey SM, McFarlane CA, Hallgren M *et al.* Psychosis prediction: 12-month follow up of a high-risk ("prodromal") group. *Schizophr Res* 2003; **60**(1)**:** 21-32.

59. Greenough MA, Volitaskis I, Li Q-X, Laughton KM, Evin G, Ho M *et al.* Presenilins Promote the Cellular Uptake of Copper and Zinc and Maintain Copper Chaperone of SOD1-dependent Copper/Zinc Superoxide Dismutase Activity. *J Biol Chem* 2011; **286**(11)**:** 9776-9786.

60. Dawson HN, Ferreira A, Eyster MV, Ghoshal N, Binder LI, Vitek MP. Inhibition of neuronal maturation in primary hippocampal neurons from tau deficient mice. *J Cell Sci* 2001; **114**(Pt 6)**:** 1179-1187.

61. Chen JC, Hardy PA, Clauberg M, Joshi JG, Parravano J, Deck JH *et al.* T2 values in the human brain: comparison with quantitative assays of iron and ferritin. *Radiology* 1989; **173**(2)**:** 521-526.

62. Bartzokis G, Garber HJ, Marder SR, Olendorf WH. MRI in tardive dyskinesia: shortened left caudate T2. *Biol Psychiatry* 1990; **28**(12)**:** 1027-1036.

63. Dhenain M, Duyckaerts C, Michot JL, Volk A, Picq JL, Boller F. Cerebral T2-weighted signal decrease during aging in the mouse lemur primate reflects iron accumulation. *Neurobiol Aging* 1998; **19**(1)**:** 65-69.

64. Positano V, Salani B, Pepe A, Santarelli MF, De Marchi D, Ramazzotti A *et al.* Improved T2* assessment in liver iron overload by magnetic resonance imaging. *Magn Reson Imaging* 2009; **27**(2)**:** 188-197.

65. Sun H, Walsh AJ, Lebel RM, Blevins G, Catz I, Lu JQ *et al.* Validation of quantitative susceptibility mapping with Perls' iron staining for subcortical gray matter. *NeuroImage* 2014.

66. Caccamo A, Oddo S, Tran LX, LaFerla FM. Lithium reduces tau phosphorylation but not A beta or working memory deficits in a transgenic model with both plaques and tangles. *Am J Pathol* 2007; **170**(5)**:** 1669-1675.

67. Malhi GS, Adams D, Berk M. Is lithium in a class of its own? A brief profile of its clinical use. *Aust NZ J Psychiatry* 2009; **43**(12)**:** 1096-1104.

68. Frank GB, Jhamandas K. Effects of drugs acting alone and in combination on the motor activity of intact mice. *Br J Pharmacol* 1970; **39**(4)**:** 696-706.

69. Healy TE, Lautch H, Hall N, Tomlin PJ, Vickers MD. Interdisciplinary study of diazepam sedation for outpatient dentistry. *Br Med J* 1970; **3**(5713)**:** 13-17.

70. Tornberg J, Segerstråle M, Kulesskaya N, Voikar V, Taira T, Airaksinen MS. KCC2-deficient mice show reduced sensitivity to diazepam, but normal alcohol-induced motor impairment, gaboxadol-induced sedation, and neurosteroid-induced hypnosis. *Neuropsychopharmacology* 2007; **32**(4)**:** 911-918.

71. Zeller A, Crestani F, Camenisch I, Iwasato T, Itohara S, Fritschy JM *et al.* Cortical glutamatergic neurons mediate the motor sedative action of diazepam. *Mol Pharmacol* 2008; **73**(2)**:** 282-291.

72. Snyder SH, Taylor KM, Coyle JT, Meyerhoff JL. The role of brain dopamine in behavioral regulation and the actions of psychotropic drugs. *The American journal of psychiatry* 1970; **127**(2)**:** 199-207.

73. Cox C, Harrison-Read PE, Steinberg H, Tomkiewicz M. Lithium attenuates drug-induced hyperactivity in rats. *Nature* 1971; **232**(5309)**:** 336-338.

74. Friedman ES, Gershon S. Effect of lithium on brain dopamine. *Nature* 1973; **243**(5409)**:** 520-521.

75. Dziedzicka-Wasylewska M, Maćkowiak M, Fijat K, Wedzony K. Adaptive changes in the rat dopaminergic transmission following repeated lithium administration. *J Neural Transm* 1996; **103**(7)**:** 765-776.

76. Atack JR, Cook SM, Watt AP, Fletcher SR, Ragan CI. In vitro and in vivo inhibition of inositol monophosphatase by the bisphosphonate L-690,330. *J Neurochem* 1993; **60**(2)**:** 652-658.

77. Meijer L, Skaltsounis AL, Magiatis P, Polychronopoulos P, Knockaert M, Leost M *et al.* GSK-3-selective inhibitors derived from Tyrian purple indirubins. *Chem Biol* 2003; **10**(12)**:** 1255-1266.

78. Zheng H, Jiang M, Trumbauer ME, Sirinathsinghji DJ, Hopkins R, Smith DW *et al.* beta-Amyloid precursor protein-deficient mice show reactive gliosis and decreased locomotor activity. *Cell* 1995; **81**(4)**:** 525-531.

79. Dallman PR, Spirito RA. Brain iron in the rat: extremely slow turnover in normal rats may explain long-lasting effects of early iron deficiency. *J Nutr* 1977; **107**(6)**:** 1075-1081.

80. Chen JH, Shahnavas S, Singh N, Ong WY, Walczyk T. Stable iron isotope tracing reveals significant brain iron uptake in adult rats. *Metallomics* 2013; **5**(2)**:** 167-173.

81. Murray N, Hopwood S, Balfour DJ, Ogston S, Hewick DS. The influence of age on lithium efficacy and side-effects in out-patients. *Psychological medicine* 1983; **13**(1)**:** 53-60.

82. Bell AJ, Cole A, Eccleston D, Ferrier IN. Lithium neurotoxicity at normal therapeutic levels. *Br J Psychiatry* 1993; **162:** 689-692.

83. Flint A. Ageing as a risk factor for lithium neurotoxicity at therapeutic serum levels. *Br J Psychiatry* 1993; **163:** 555-556.

84. Hare D, Ayton S, Bush A, Lei P. A delicate balance: Iron metabolism and diseases of the brain. *Front Aging Neurosci* 2013; **5:** 34.

85. Hajek T, Kopecek M, Hoschl C, Alda M. Smaller hippocampal volumes in patients with bipolar disorder are masked by exposure to lithium: a meta-analysis. *J Psychiatry Neurosci* 2012; **37**(5)**:** 333-343.

86. Pfennig A, Alda M, Young T, MacQueen G, Rybakowski J, Suwalska A *et al.* Prophylactic lithium treatment and cognitive performance in patients with a long history of bipolar illness: no simple answers in complex disease-treatment interplay. *International journal of bipolar disorders* 2014; **2:** 1.

87. Wingo AP, Wingo TS, Harvey PD, Baldessarini RJ. Effects of lithium on cognitive performance: a meta-analysis. *The Journal of clinical psychiatry* 2009; **70**(11)**:** 1588-1597.

88. Mora E, Portella MJ, Forcada I, Vieta E, Mur M. Persistence of cognitive impairment and its negative impact on psychosocial functioning in lithium-treated, euthymic bipolar patients: a 6-year follow-up study. *Psychological medicine* 2013; **43**(6)**:** 1187-1196.

89. Evrensel A, Unsalver BO, Ceylan ME, Comert G. Lithium-induced cortical atrophy and cognitive dysfunction. *BMJ case reports* 2014; **2014**.

90. Wang X, Culotta VC, Klee CB. Superoxide dismutase protects calcineurin from inactivation. *Nature* 1996; **383**(6599)**:** 434-437.

91. Namgaladze D, Hofer HW, Ullrich V. Redox control of calcineurin by targeting the binuclear Fe(2+)-Zn(2+) center at the enzyme active site. *J Biol Chem* 2002; **277**(8)**:** 5962-5969.

92. Huang C, Li J, Zhang Q, Huang X. Role of bioavailable iron in coal dust-induced activation of activator protein-1 and nuclear factor of activated T cells: difference between Pennsylvania and Utah coal dusts. *Am J Respir Cell Mol Biol* 2002; **27**(5)**:** 568-574.

93. Huang X, Dai J, Huang C, Zhang Q, Bhanot O, Pelle E. Deferoxamine synergistically enhances iron-mediated AP-1 activation: a showcase of the interplay between extracellular-signal-regulated kinase and tyrosine phosphatase. *Free radical research* 2007; **41**(10)**:** 1135-1142.

94. Kremer A. GSK3 and Alzheimer's disease: facts and fiction…. *Front Mol Neurosci* 2011; **4:** 1-10.

95. Hu S, Begum AN, Jones MR, Oh MS, Beech WK, Beech BH *et al.* GSK3 inhibitors show benefits in an Alzheimer's disease (AD) model of neurodegeneration but adverse effects in control animals. *Neurobiology of disease* 2009; **33**(2)**:** 193-206.

96. Gómez-Sintes R, Hernández F, Bortolozzi A, Artigas F, Avila J, Zaratin P *et al.* Neuronal apoptosis and reversible motor deficit in dominant-negative GSK-3 conditional transgenic mice. *EMBO J* 2007; **26**(11)**:** 2743-2754.

97. Ayton S, Lei P. The Abeta-induced NFAT apoptotic pathway is also activated by GSK-3 inhibition: implications for Alzheimer therapeutics. *J Neurosci* 2012; **32**(28)**:** 9454-9456.

98. Macdonald A, Briggs K, Poppe M, Higgins A, Velayudhan L, Lovestone S. A feasibility and tolerability study of lithium in Alzheimer's disease. *Int J Geriatr Psychiatry* 2008; **23**(7)**:** 704-711.

99. Aggarwal SP, Zinman L, Simpson E, Mckinley J, Jackson KE, Pinto H *et al.* Safety and efficacy of lithium in combination with riluzole for treatment of amyotrophic lateral sclerosis: a randomised, double-blind, placebo-controlled trial. *Lancet neurology* 2010; **9**(5)**:** 481-488.

100. Swash M. Lithium time-to-event trial in amyotrophic lateral sclerosis stops early for futility. *Lancet neurology* 2010; **9**(5)**:** 449-451.

101. Verstraete E, Veldink JH, Huisman MH, Draak T, Uijtendaal EV, van der Kooi AJ *et al.* Lithium lacks effect on survival in amyotrophic lateral sclerosis: a phase IIb randomised sequential trial. *Journal of neurology, neurosurgery, and psychiatry* 2012; **83**(5)**:** 557-564.

102. Ayton S, Lei P, Bush AI. Biometals and Their Therapeutic Implications in Alzheimer's Disease. *Neurotherapeutics : the journal of the American Society for Experimental NeuroTherapeutics* 2014.

103. Langkammer C, Enzinger C, Quasthoff S, Grafenauer P, Soellinger M, Fazekas F *et al.* Mapping of iron deposition in conjunction with assessment of nerve fiber tract integrity in amyotrophic lateral sclerosis. *Journal of magnetic resonance imaging : JMRI* 2010; **31**(6)**:** 1339-1345.

104. Oba H, Araki T, Ohtomo K, Monzawa S, Uchiyama G, Koizumi K *et al.* Amyotrophic lateral sclerosis: T2 shortening in motor cortex at MR imaging. *Radiology* 1993; **189**(3)**:** 843-846.

Figure legends

Figure 1. T_2 relaxation time reductions in the SN of participants treated with lithium. a) Representative MRI images from treatment as usual (top) and lithium (bottom) ultra high risk groups. Arrow indicates the SN. **b**) Significant reduction in T_2 relaxation time was found in lithium-treated subjects ($p<0.001$ compared to treatment as usual controls; $p=0.007$ compared to pre-treated scan, two-tailed t-test). Dotted line indicates values of baseline scan. n[treatment as usual]=9, n[lithium]=11. Means ± SEM are shown. *** $p<0.001$ (versus treatment as usual), ## $p<0.01$ (versus pre-scan).

Figure 2. Lithium induces brain iron elevation and parkinsonism in mice. a) Lithium treatment did not induce a change in mouse weight, monitored daily as an index of animal health. **b**) Lithium treatment elevated levels in mouse brain and liver ($p<0.001$ for Ctx, SN, Cereb, or Liver, two-tailed t-test). **c**) Li treatment induced iron elevation in cerebral regions ($p=0.008$ for cortex, Ctx; $p=0.039$ for SN; two-tailed t-test) but not cerebellum (Cereb), liver, or plasma. **d**) Iron levels in SN correlate with lithium levels in Li-treated mice ($R^2=0.62$, $p=0.007$, linear regression) but not sham-treated mice ($R^2=0.02$, $p=0.702$, linear regression).**e**) Quantification of western blots showed reduction of tau in cortex ($p=0.032$, two-tailed t-test) and SN ($p<0.001$, two-tailed t-test) of Li-treated mice compared to sham-treated mice. **f**) Following 21 days exposure, Li-treated mice took longer to turn ($p=0.008$, two-tailed t-test) in the Pole test. **g**) Li-treated mice maintained less time on the rod compared to sham-treated mice ($p=0.004$, two-tailed t-test). n=12 per treatment group. **h-i**) Representative TH-staining of sham- (top) and Li- (bottom) treated mice. Quantitative data are shown in **i**. Significant reduction was found in TH-ir neurons in the SN of Li-treated mice ($p<0.001$, two-tailed t-test). n=5 per treatment group. **j**)

Significant reductions were found in the striatal dopamine levels (p=0.023, two-tailed t-test), measured by HPLC in Li-treated mice. n=12 per treatment group. Means ± SEM are shown. * p<0.05, ** p<0.01, *** p<0.001.

Figure 3. Li-induced iron elevation is caused by tau reduction in primary neuronal culture. **a**) Li treatment to neurons for 18 h induced dose-dependent ^{59}Fe retention (p=0.005 for 5mM Li, p<0.001 for 10mM Li, one-way ANOVA, n=4 per treatment). **b**) Li treatment of neurons for 18h induced specific iron elevation (p<0.001, two-tailed t-test, n=6 per treatment), without altering copper or zinc. **c**) Li treatment (10 mM) inhibited iron export (p<0.001, non-linear regression with extra sum-of-squares F test, n=6 per group). **d**) Li treatment reduced neuronal tau levels (representative blots shown beneath) at 5mM (p=0.007) and 10mM (p=0.034, one-way ANOVA) after 18 h. n=4 per group. **e**) Tau knockout neurons retained more ^{59}Fe iron (p=0.032) (18 h), but, in contrast to wild type neurons, were resistant to Li-induced iron accumulation (p=0.038, two-way ANOVA). n=4 per group. Each experiment was independently repeated three times. Means ± SEM are shown. * p<0.05, ** p<0.01, *** p<0.001.

Figure 4. Li-induced parkinsonism is mediated by tau and APP. a) Daily mean weights of the mouse cohorts revealed no significant impact of lithium treatment within each genotype group during the course of study. APP knockout mice were lighter, as reported previously[78]. **b**) Li treatment significantly elevated plasma lithium levels of 3-month-old wild type (p<0.001, Two-way ANOVA with post-hoc Dunnett's test), tau knockout (p<0.001), and APP knockout (p=0.007) mice. These concentrations are well below the usual therapeutic range of clinical lithium therapy. **c-d**) Elevated iron levels were observed in the cortex (**c**, p=0.031, two-way ANOVA with post-hoc Dunnett's test) and SN (**d**, p=0.041) of Li-treated wild type mice, but

loss of tau or APP abolished the elevation. **e-f**) Li treatment induced tau reduction in cortex and SN of both wild type (**e**, p=0.041 for cortex, p<0.001 for SN, two-tailed t-test) and APP knockout mice (**f**, p=0.006 for cortex, p=0.041 for SN, two-tailed t-test). **g-h**) Li-treated wild type mice required longer time to turn in the Pole test (**g**, p=0.020, two-way ANOVA with post-hoc Dunnett's test) and showed significantly reduced average distance per movement in the Open field test (**h**, p<0.001), but loss of tau or APP protected against Li-induced motor impairment. **i**) Li treatment caused SN dopaminergic neuron loss (p<0.001, two-way ANOVA with post-hoc Dunnett's test), but did not cause similar neuronal loss in tau knockout or APP knockout mice. **j**) Li treatment impaired cognitive function of wild type mice, evidenced by significantly reduced novel arm duration in the Y maze test (p=0.022, two-tailed t-test). Such impairment was not evident in tau knockout and APP knockout mice. **k**) Representative coronal section of cerebrum of wild type mice treated with sham (left) or Li (right). Arrow indicates the landmark used to identify the section. Lines indicate the area quantified. **l**) Significant enlargement of LV was found in Li-treated wild type mice (p=0.023, two-way ANOVA with post-hoc Dunnett's test), but not in Li-treated tau knockout or APP knockout mice. n=9-11 per treatment group. Means ± SEM are shown. * p<0.05, ** p<0.01, *** p<0.001.

Figure 5. A model of affected pathways for lithium-induced neurodegeneration. Lithium treatment suppresses soluble tau protein levels, which prevents APP trafficking to the neuronal surface. Lack of surface APP destabilizes ferroportin (Fpn), which results in iron accumulation. Elevated iron activates calcineurin/NFAT/Fas signaling, which then induces neuronal apoptosis, engendering motor and cognitive disability.

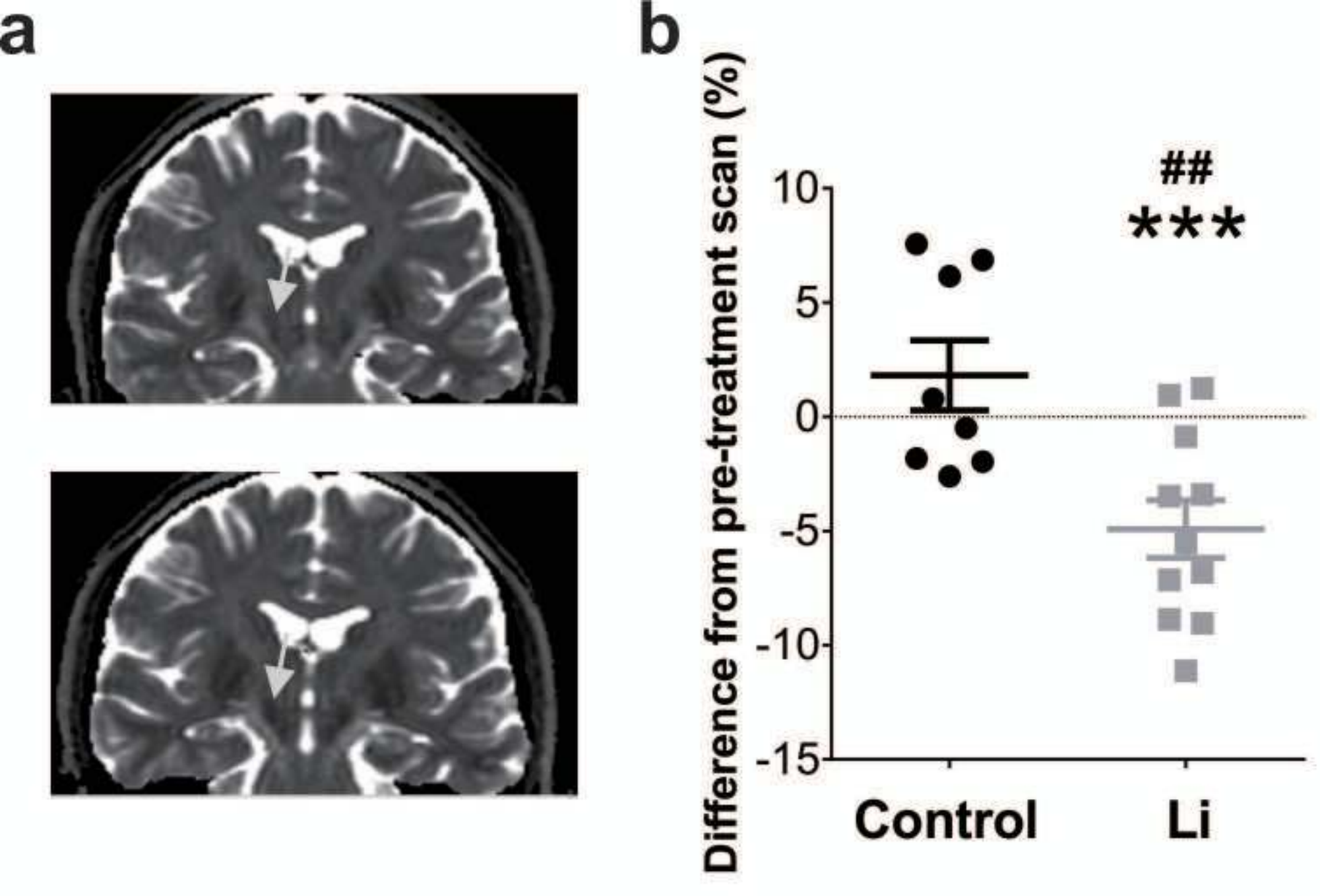
a
b
Difference from pre-treatment scan (%)
10
5
0
-5
-10
-15
##
***
Control
Li

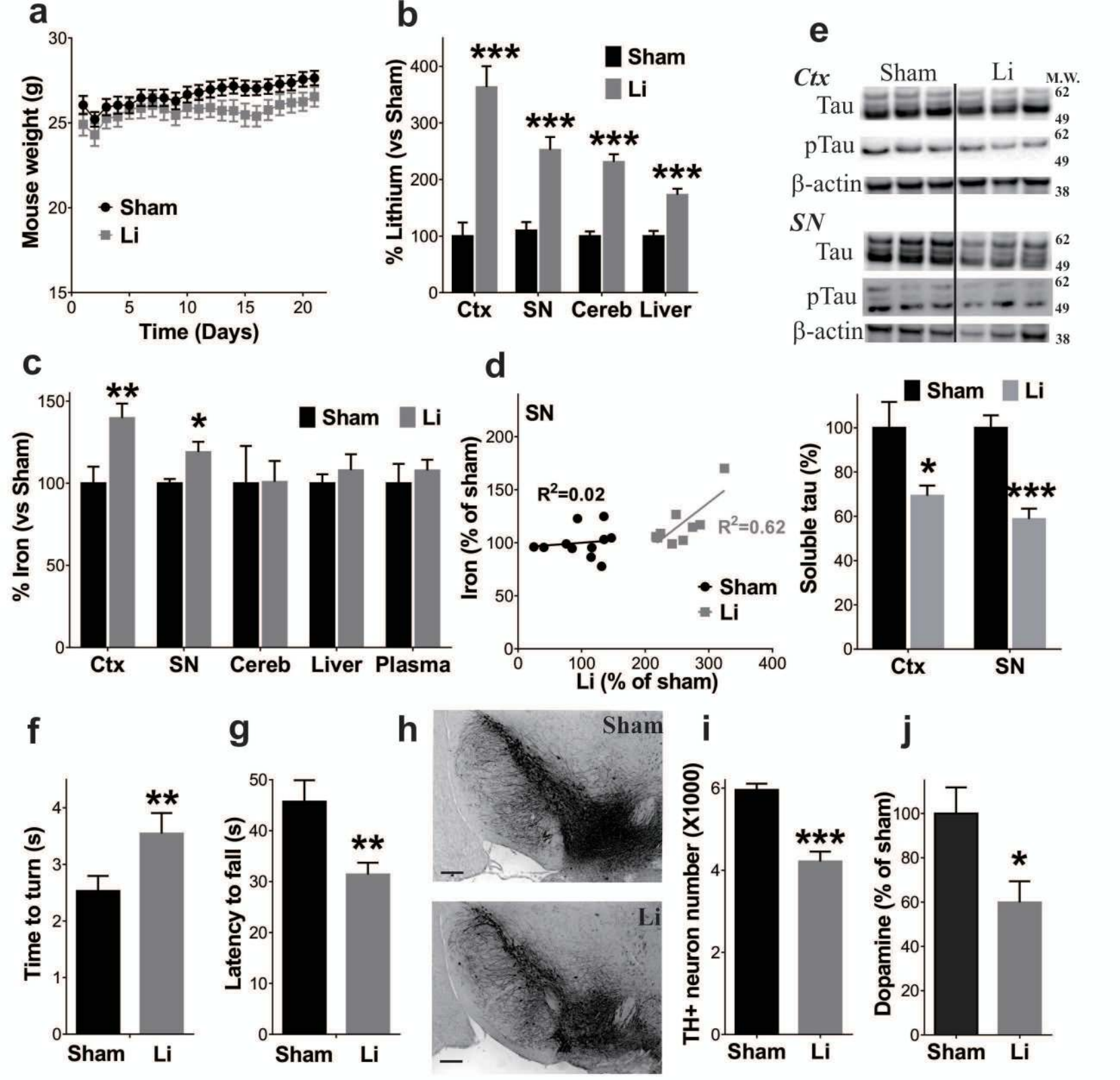
a
Mouse weight (g)
Time (Days)
Sham
Li
b
% Lithium (vs Sham)
Sham
Li
***
Ctx
SN
Cereb
Liver
e
Ctx
Sham
Li
M.W.
Tau
pTau
β-actin
SN
62
49
38
c
% Iron (vs Sham)
**
*
Sham
Li
Ctx
SN
Cereb
Liver
Plasma
d
SN
Iron (% of sham)
R2=0.02
R2=0.62
Sham
Li
Li (% of sham)
Soluble tau (%)
Sham
Li
*
***
Ctx
SN
f
Time to turn (s)
**
Sham
Li
g
Latency to fall (s)
**
Sham
Li
h
Sham
Li
i
TH+ neuron number (X1000)
***
Sham
Li
j
Dopamine (% of sham)
*
Sham
Li

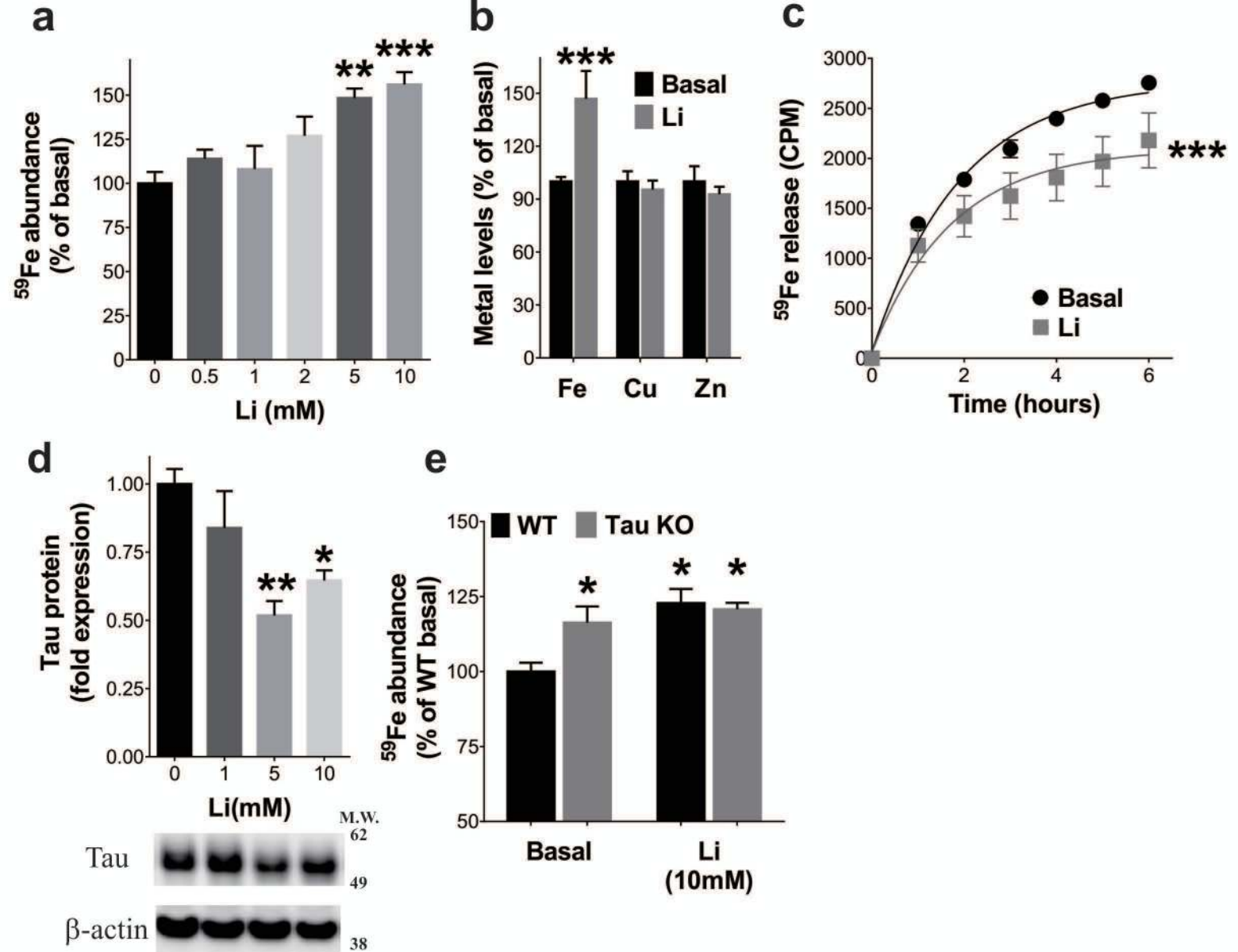
a
^{59}Fe abundance (% of basal)
150
125
100
75
50
25
0
**
***
0
0.5
1
2
5
10
Li (mM)
b
Metal levels (% of basal)
150
120
90
60
30
0
***
Basal
Li
Fe
Cu
Zn
c
^{59}Fe release (CPM)
3000
2500
2000
1500
1000
500
0
***
Basal
Li
0
2
4
6
Time (hours)
d
Tau protein (fold expression)
1.00
0.75
0.50
0.25
0.00
**
*
0
1
5
10
Li(mM)
M.W.
62
49
Tau
β-actin
38
e
^{59}Fe abundance (% of WT basal)
150
125
100
75
50
WT
Tau KO
*
*
*
Basal
Li (10mM)

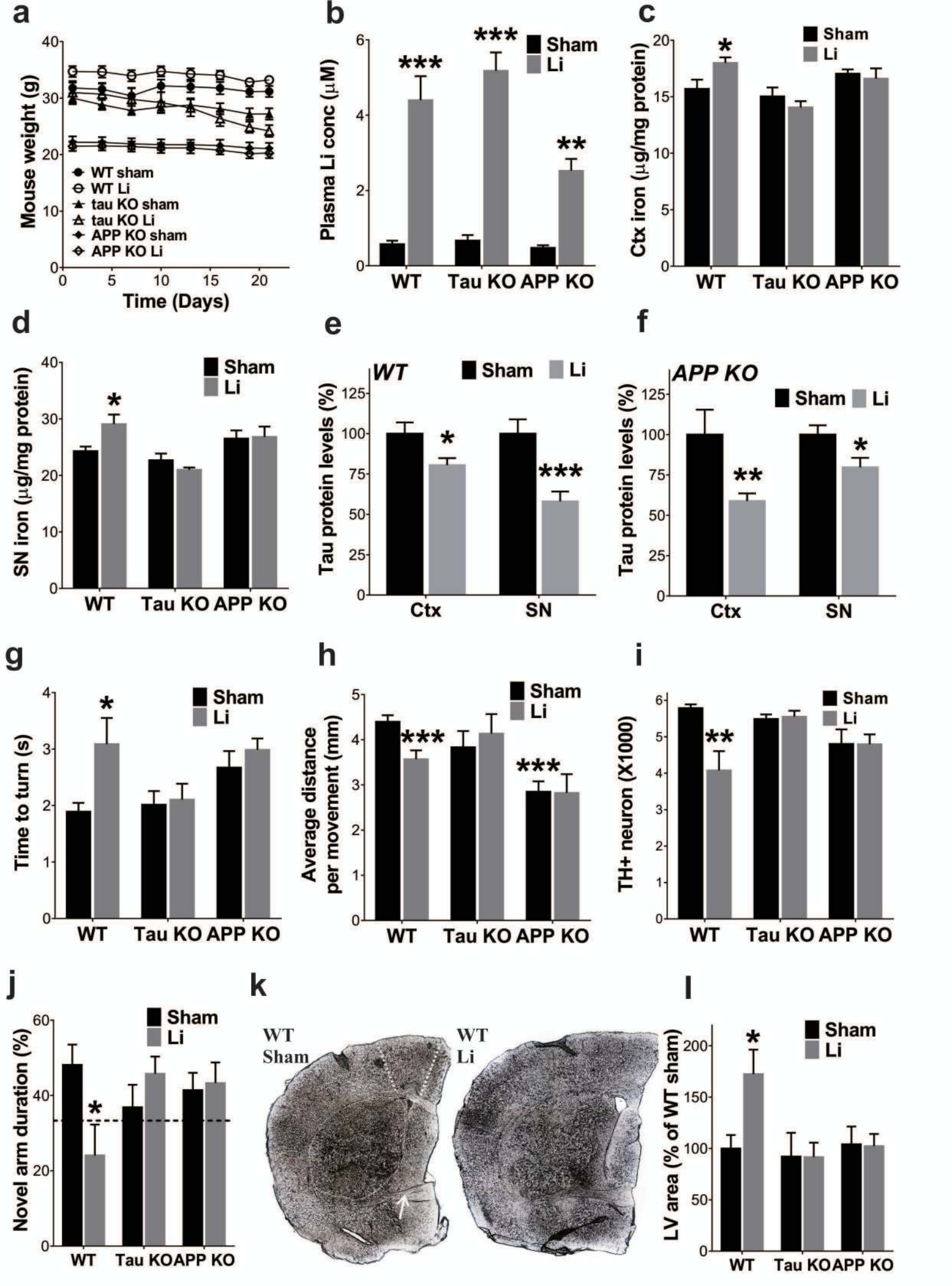
a
Mouse weight (g)
Time (Days)
WT sham
WT Li
tau KO sham
tau KO Li
APP KO sham
APP KO Li
b
Plasma Li conc (μM)
Sham
Li
WT
Tau KO
APP KO
c
Ctx iron (μg/mg protein)
d
SN iron (μg/mg protein)
e
WT
Tau protein levels (%)
Ctx
SN
f
APP KO
g
Time to turn (s)
h
Average distance per movement (mm)
i
TH+ neuron (X1000)
j
Novel arm duration (%)
k
WT Sham
WT Li
l
LV area (% of WT sham)

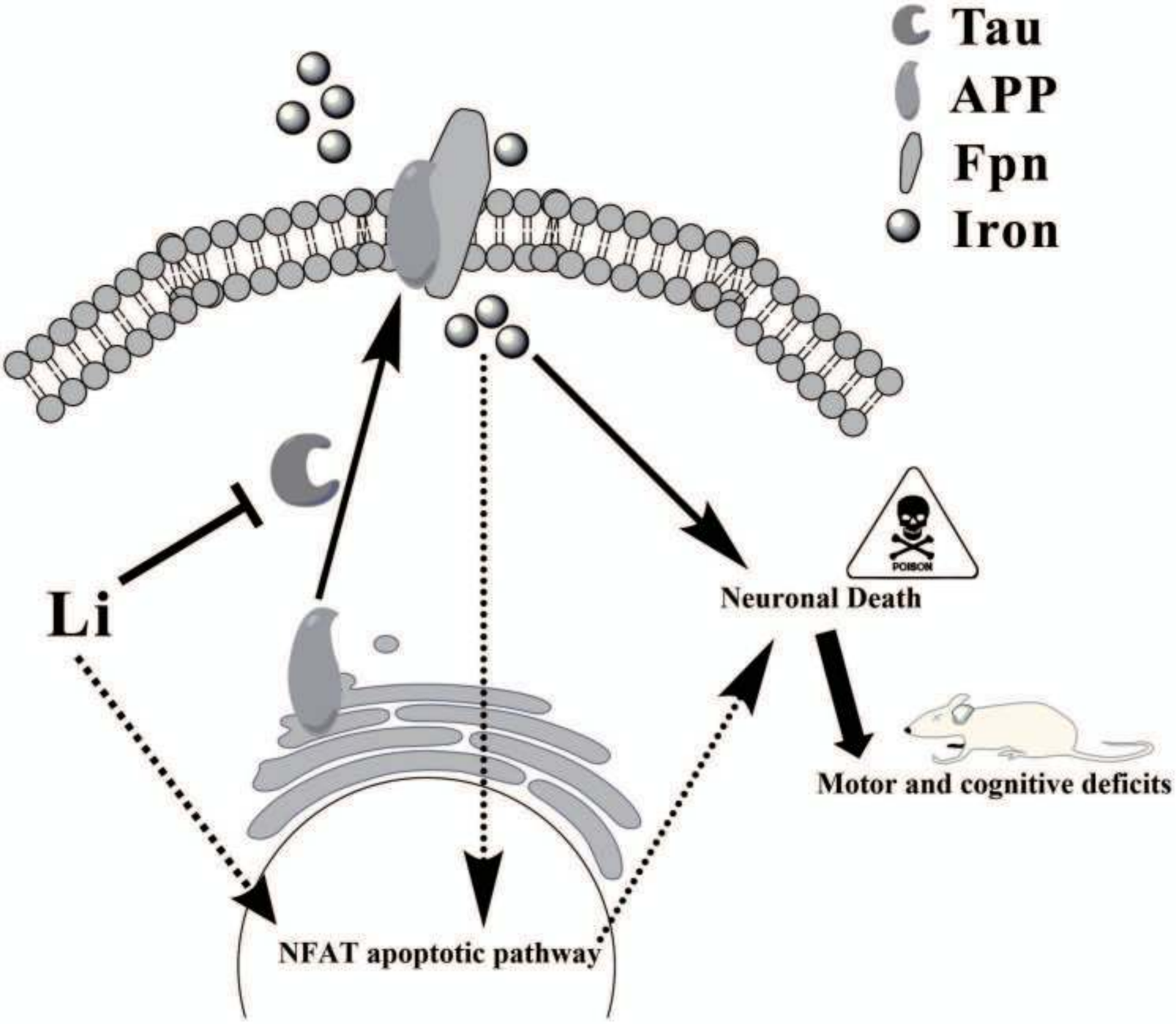
Tau
APP
Fpn
Iron
Li
POISON
Neuronal Death
Motor and cognitive deficits
NFAT apoptotic pathway

Supplementary Information

Lithium suppression of tau induces brain iron accumulation and neurodegeneration

Peng Lei, Scott Ayton, Ambili Thoppuvalappil Appukuttan, Steve Moon, James A. Duce, Irene Volitakis, Robert Cherny, Stephen J. Wood, Mark Greenough, Gregor Berger, Christos Pantelis, Patrick McGorry, Alison Yung, David I. Finkelstein, and Ashley I. Bush

Inventory of Supplementary Information.

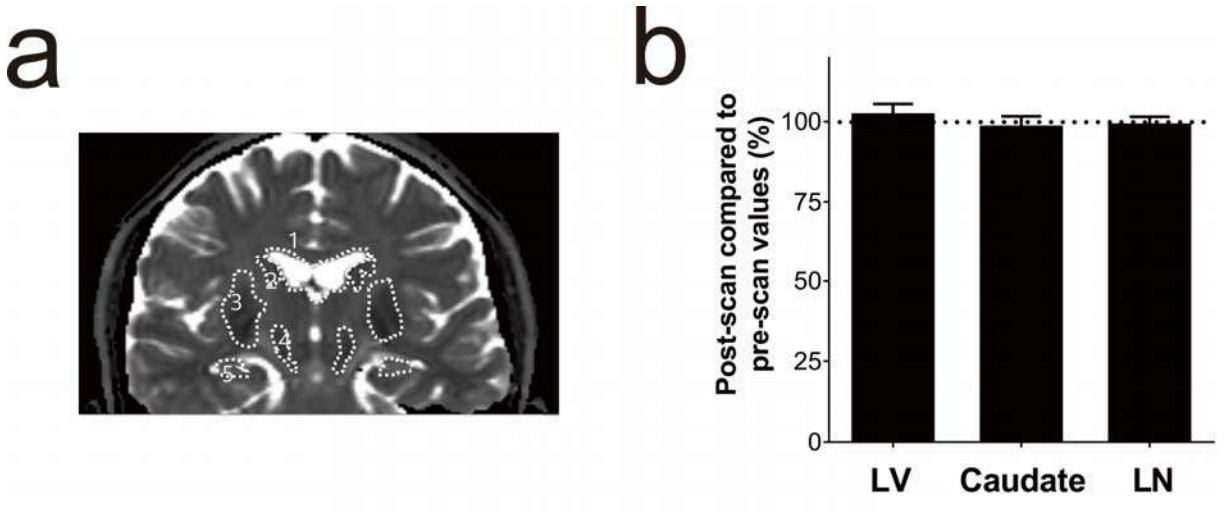

Supplementary Figure 1. T_2 relaxation time in brain regions from subjects treated with lithium. **a**) Regions of interest were mapped as illustrated by an operator blinded to treatment group. 1. lateral ventricular area (LV); 2. Caudate; 3. lenticular nucleus (LN); 4. SN; 5. Hippocampus (previously reported[1]). **b**) No change in T_2 relaxation time was found in the Caudate and LN of lithium-treated participants (p=0.18 for Caudate; p=0.29 for LN, two-tailed t-test). LV area was unaltered by Li treatment (p=0.177, two-tailed t-test). n[treatment as usual]=9, n[lithium]=11. Means ± SEM are shown.

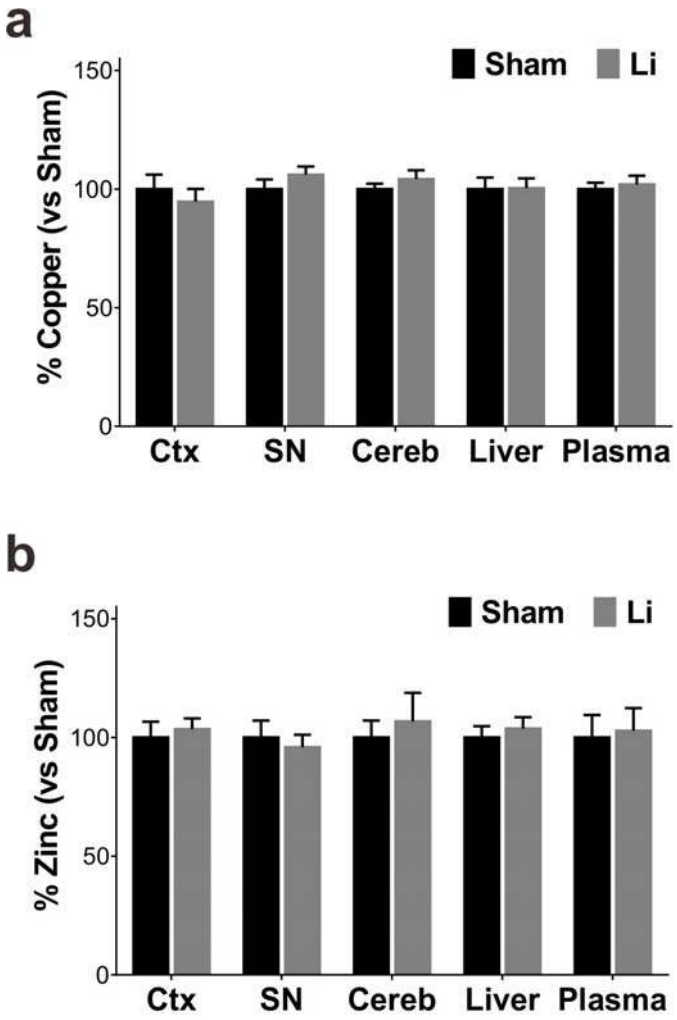

Supplementary Figure 2. No changes in copper (**a**) or zinc (**b**) levels in tissues of Li-treated mice. Means ± SEM are shown, n=12 per treatment group.

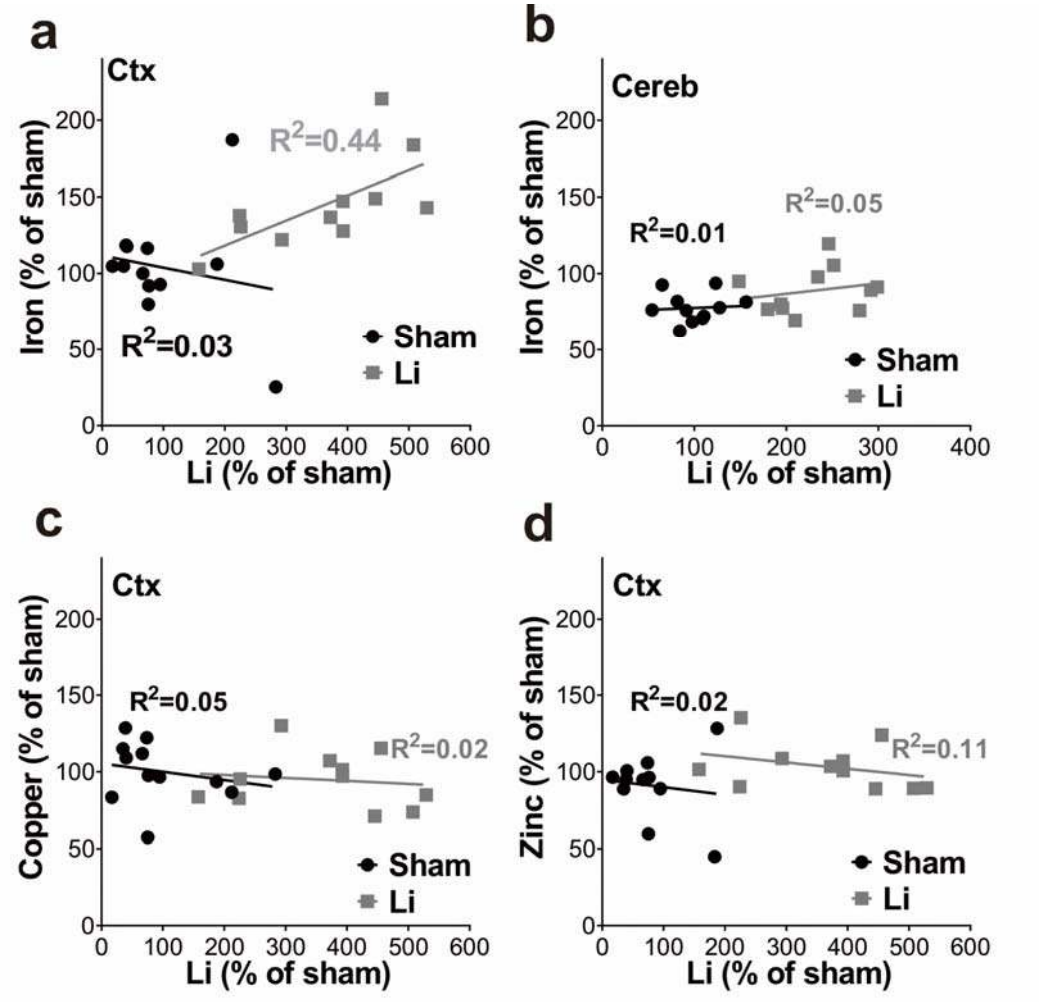

Supplementary Figure 3. Correlations between bio-metals and Li in brain regions of Li-treated and sham-treated mice. **a)** Iron levels in cortex correlates with lithium levels in Li-treated mice (R^2=0.439, p=0.026, linear regression) but not sham-treated mice (R^2=0.0327, p=0.574, linear regression). **b**) No correlation between iron and lithium levels in cerebellum. **c-d**) No correlation between copper (**c**) or zinc (**d**) and lithium levels in cortex. n=12 per treatment group.

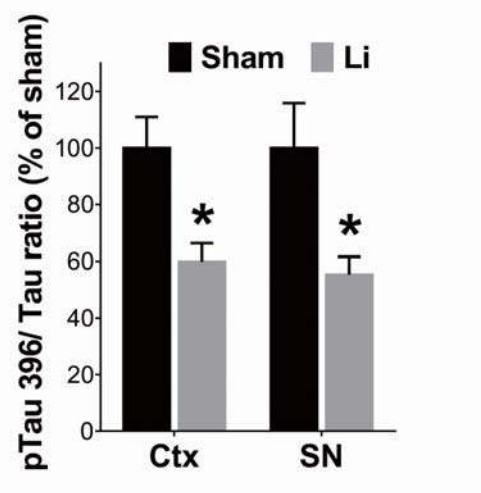

Supplementary Figure 4. Li treatment reduces phosphorylated tau levels in both cortex and SN. Quantification of western blot showed reduction of tau phosphorylation at Ser396 in cortex (p=0.034, two-tailed t-test) and SN (p=0.039, two-tailed t-test) of Li-treated mice compared to sham-treated mice. Means ± SEM are shown, n=12 per treatment group. * p<0.05.

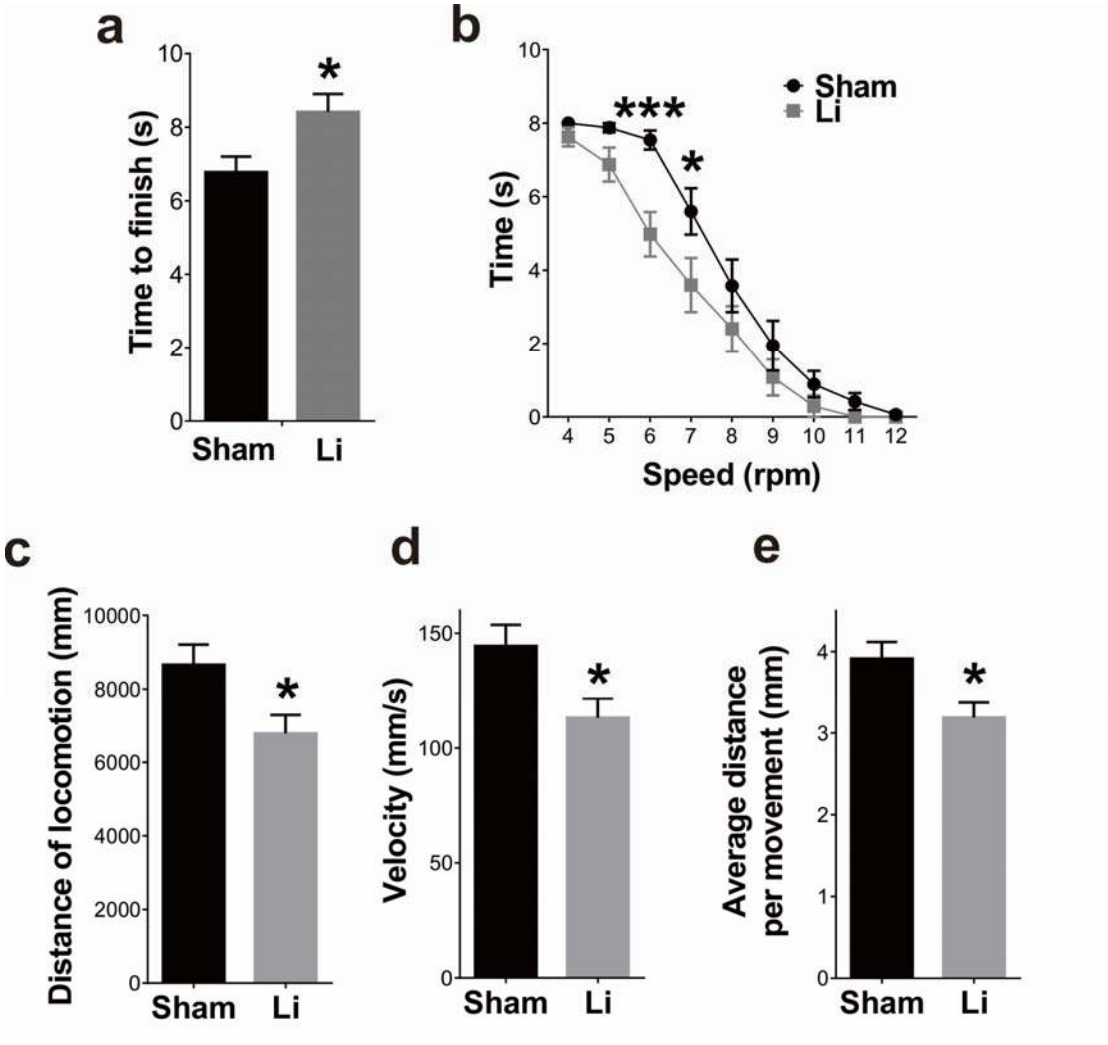

Supplementary Figure 5. Additional locomotor deficits induced by Li treatment. **a**) Li-treated mice required longer time to finish (p=0.041, two-tailed t-test) in the Pole test after 21 days of treatment. **b**) Li-treated mice showed reduced maximum speed in the Rotarod test. Two-way ANOVA with post-hoc Dunnett's test: speed (p< 0.001), and treatment (p< 0.001) effects but no interaction (p = 0.107). **c-e**) Li-treated mice showed reduced distance of locomotion (**c**, p=0.022, two-tailed t-test), reduced velocity (**d**, p=0.023), and reduced average distance per movement (**e**, p=0.018) in the Open field test. Means ± SEM are shown, n=12 per treatment group. * p<0.05, *** p<0.001.

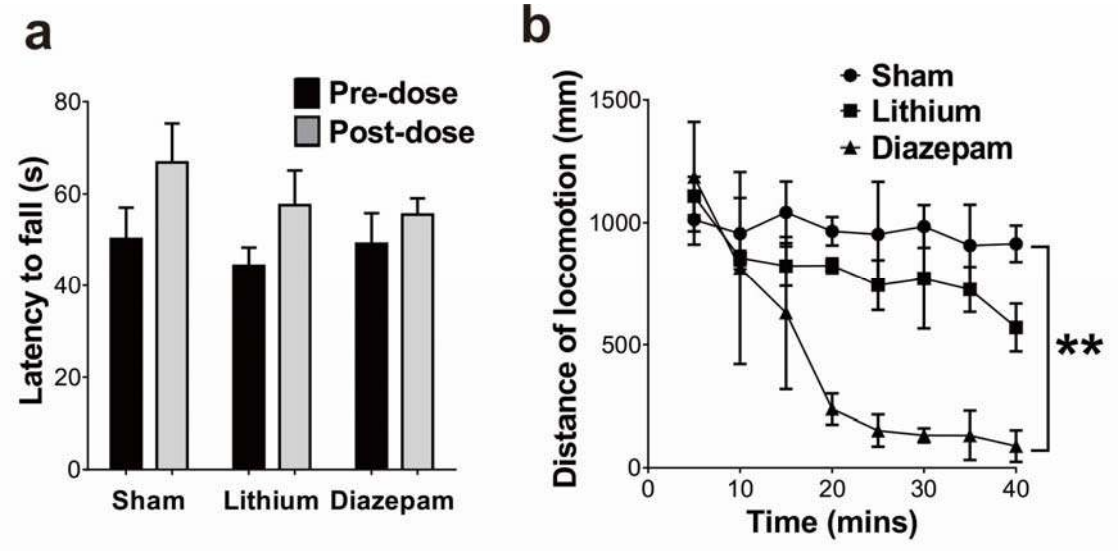

Supplementary Figure 6. Li-induced motor impairment is independent of its sedative effect. **a**) Neither a single dose of Li (3.6mg/kg, gavage) nor diazepam (3mg/kg, gavage) significantly altered the performance of mice in the Rotarod test 2 hours post-dose. **b**) Diazepam sedated mice within 20 minutes, evidenced by decreased locomotion in the Open field test 20 minutes after the dose was delivered, however no such effect was found following the lithium dose. Means ± SEM are shown, n=5 per treatment group. Both experiments tested for significance with two-way ANOVA and post-hoc Dunnett's test. ** p=0.0064.

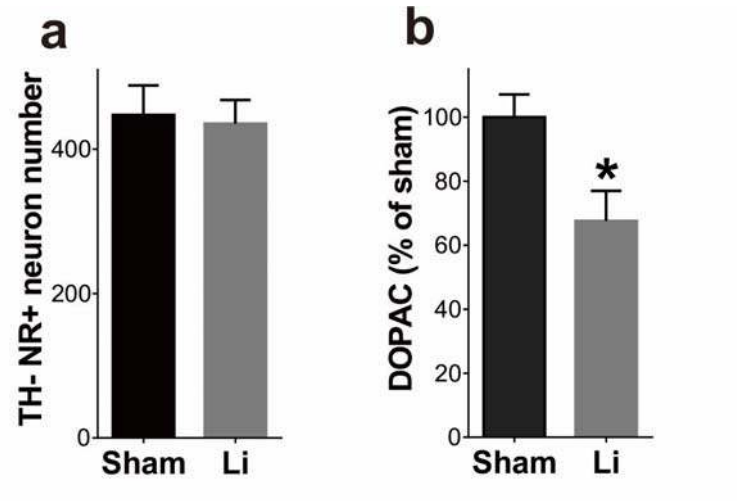

Supplementary Figure 7. Li treatment selectively affects dopaminergic neurons in the SN. a) No significant reduction (p=0.821, two-tailed t-test) was found in TH-negative, Neutral Red-positive neurons in the SN of Li-treated mice. n=5 per treatment group. b) Significant reductions were found in the striatal DOPAC levels (p=0.024, two-tailed t-test). n=12 per treatment group. Means ± SEM are shown. * p<0.05.

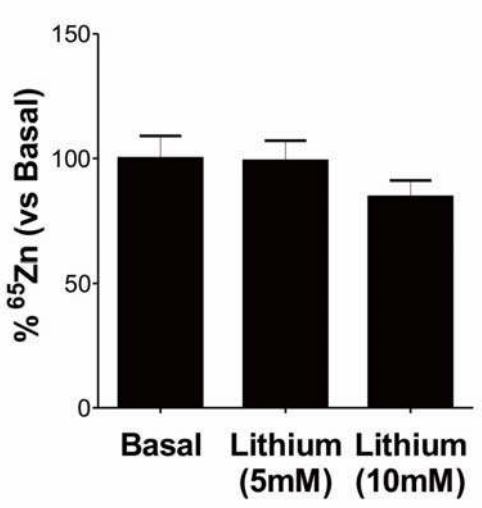

Supplementary Figure 8. Lithium treatment does not alter ^{65}Zn retention in primary neurons (p=0.176 for 10mM Li, two-tailed t-test). Means ± SEM are shown, n=4 per group.

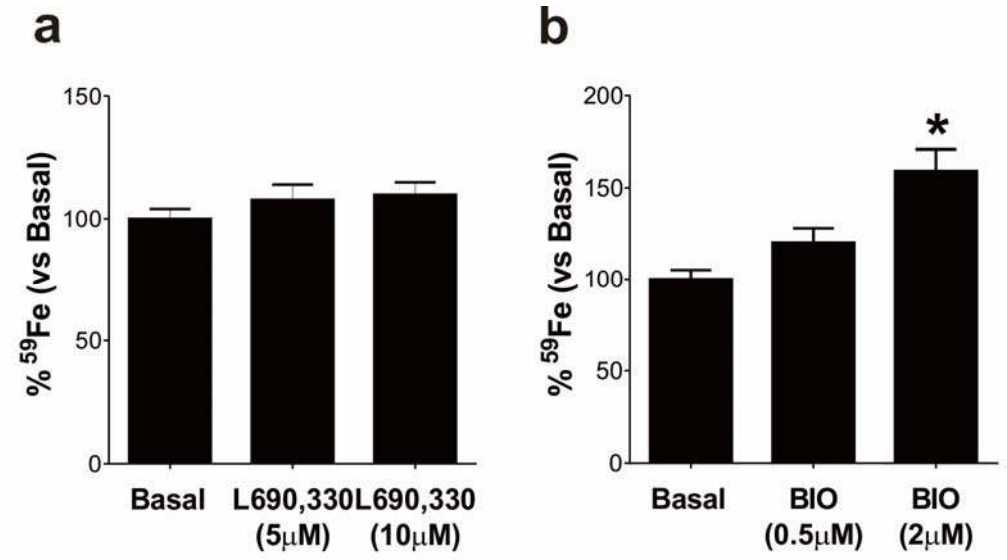

Supplementary Figure 9. Iron accumulation is induced GSK-3 inhibition. **a**) No ^{59}Fe retention was found after L690,330 (p=0.106, one-way ANOVA with post-hoc Dunnett's test) treatment. **b**) Significant ^{59}Fe retention was found after BIO treatment (p=0.002, one-way ANOVA with post-hoc Dunnett's test). Each experiment was independently repeated three times. Means ± SEM are shown, n=4 per group. * p<0.05.

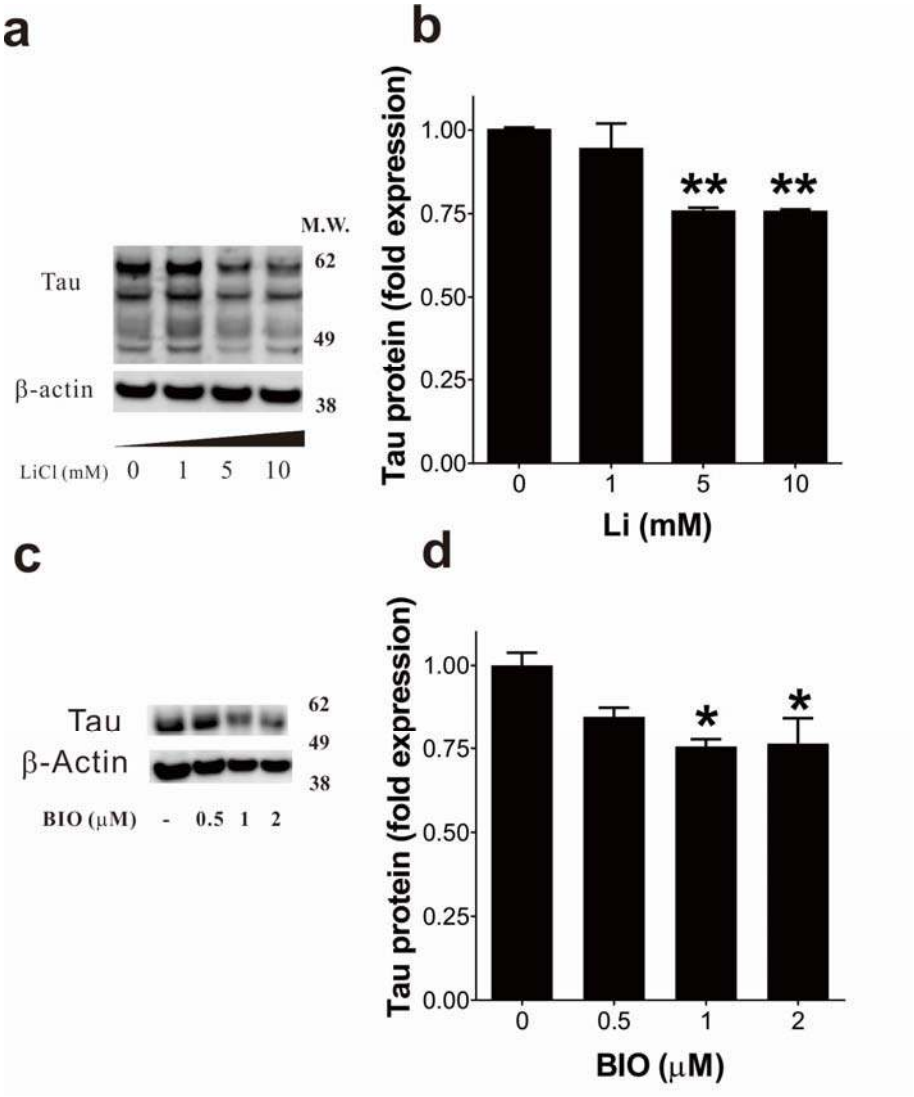

Supplementary Figure 10. Li and BIO (18h incubation) suppress tau protein levels. **a**) Representative tau western blots from lithium-treated SH-SY5Y cells. **b**) Quantification of (**a**) showed lowering of tau with 5 mM (p=0.003, one-way ANOVA with post-hoc Dunnett's test) or 10 mM (p=0.002) Li treatment. **c**) Representative western blot for tau from BIO-treated primary neurons. **d**) Quantification of (**c**) showed that BIO lowered tau levels (p=0.043 for 1 μM and p=0.048 for 2 μM, one-way ANOVA with post-hoc Dunnett's test). Means ± SEM are shown, n=4 per group, and the experiments were independently repeated three times. * p<0.05, ** p<0.01.

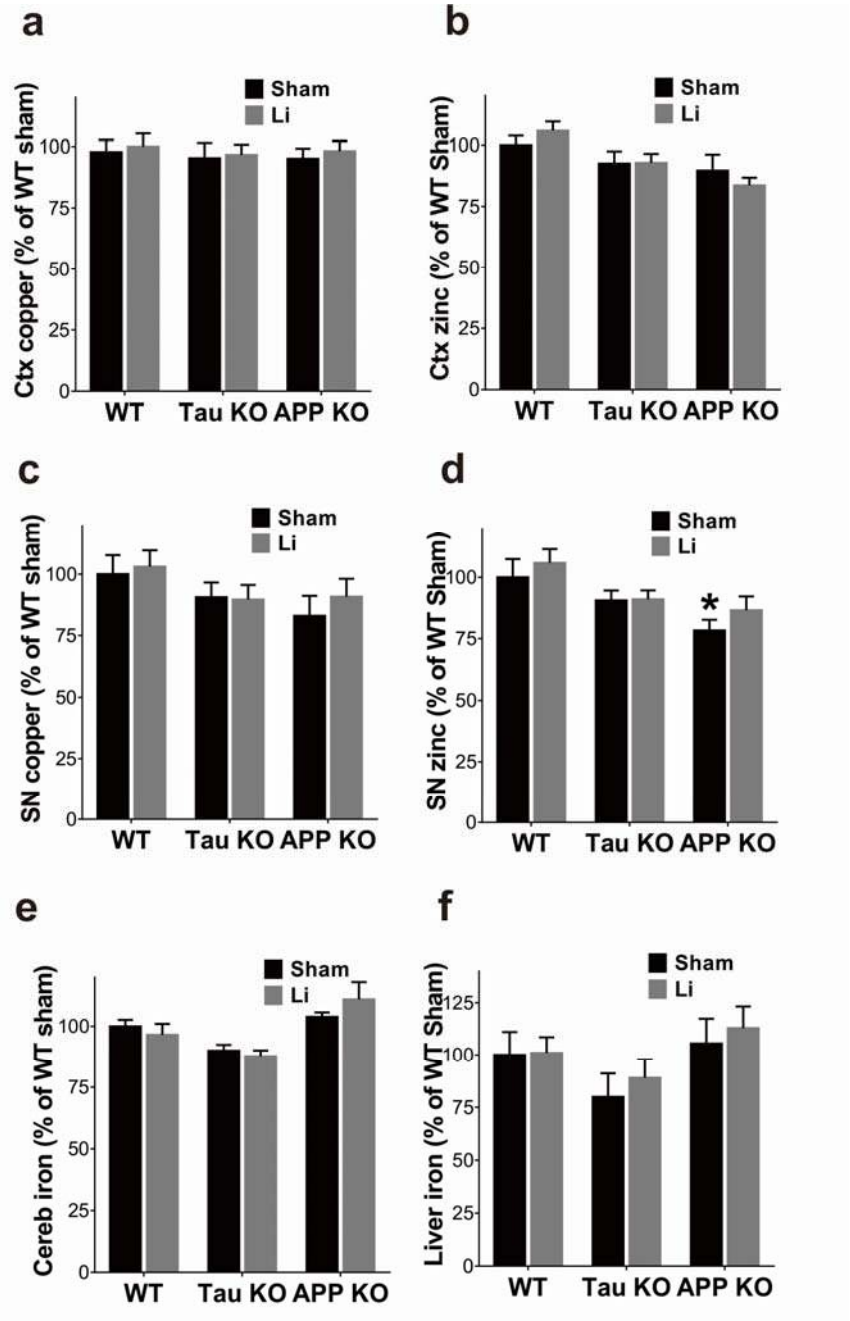

Supplementary Figure 11. No changes in (**a**) cortex copper, (**b**) cortex zinc, (**c**) SN copper, (**d**) SN zinc, (**e**) cerebellum iron, or (**f**) liver iron levels in tissues of Li-treated mice, regardless of genotype. Means ± SEM are shown, n=9-11 per treatment group.

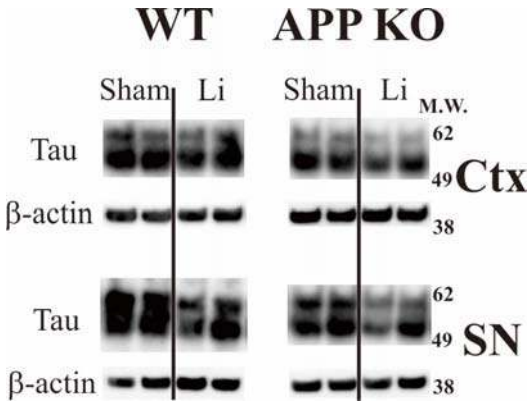

Supplementary Figure 12. Representative western blot images of cortex and SN tau protein in wild type and APP knockout mice.

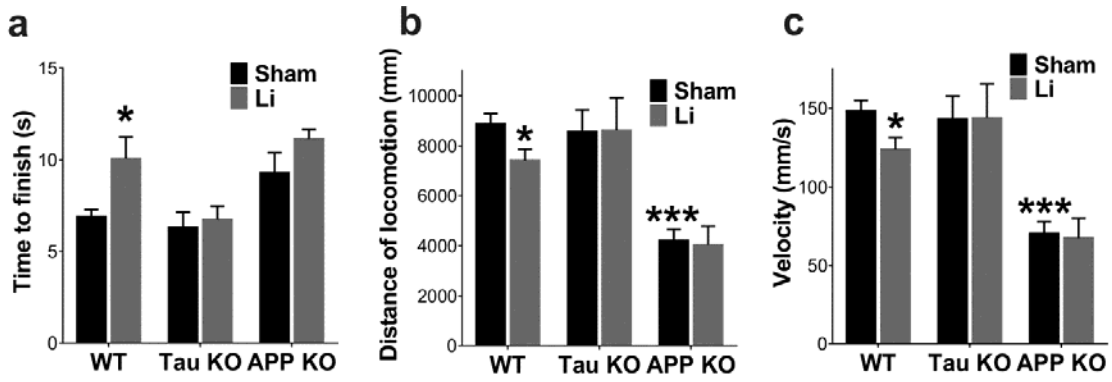

Supplementary Figure 13. Additional motor deficits in wild type mice induced by Li treatment. **a-c**) Li-treated wild type mice required longer time to finish [**a**; two-way ANOVA with post-hoc Dunnett's test: genotype (p= 0.014), and treatment (p< 0.001) effects but no interaction (p= 0.283)] in the Pole test, showed reduced distance of locomotion [**b**; genotype (p< 0.001), but no treatment (p= 0.368) effects nor interaction (p= 0.501)], and reduced velocity [**c**; genotype (p< 0.001), but no treatment (p= 0.361) effects nor interaction (p= 0.500)] in the Open field test, but loss of tau or APP protected against Li-induced motor impairment. APP knockout mice showed motor deficits themselves, evidenced by reduced distance of locomotion (p< 0.001), and reduced velocity (p< 0.001). Li treatment did not further worsen the phenotype. Means ± SEM are shown, n=9-11 per treatment group. * p<0.05, *** p<0.001.

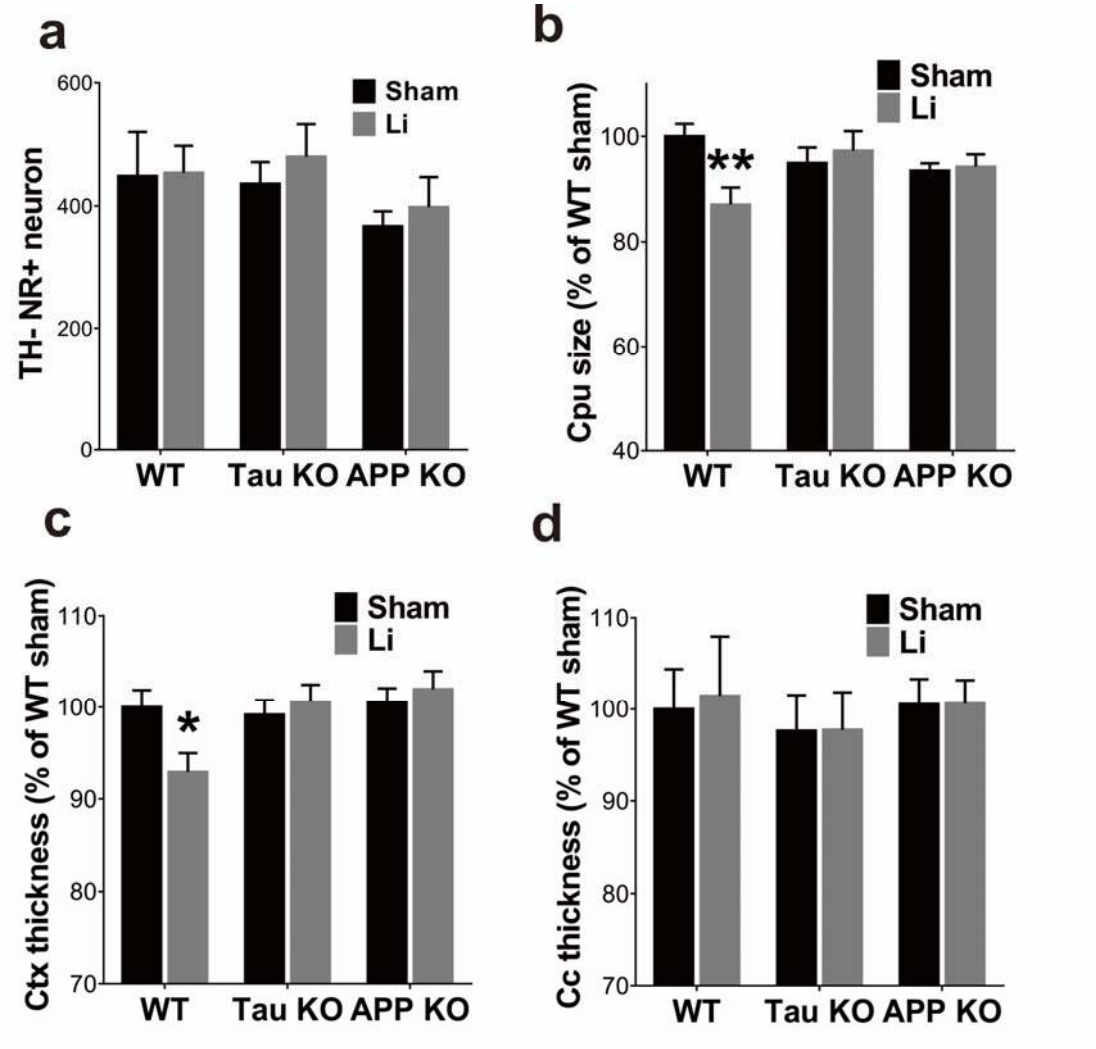

Supplementary Figure 14. Other neuroanatomical changes induced by Li. **a**) No significant reduction was found in TH-negative, Neutral Red-positive neurons in the SN of Li-treated mice. **b-c**) Li treatment reduced CPu size [**b**; two-way ANOVA with post-hoc Dunnett's test: no genotype (p= 0.606) or treatment (p= 0.153) effects, but interaction (p= 0.017)] and cortical thickness [**c**; genotype (p= 0.041) and interaction (p= 0.043) effects, but no treatment (p= 0.371) effect] in wild type mice, but the effect was abolished by loss of tau or APP. **d**) No change in corpus callosum thickness was detected in all three mouse strains. Means ± SEM are shown, n=9-11 per treatment group. * p<0.05, ** p<0.01.

Reference

1. Gómez-Sintes R, Lucas JJ. NFAT/Fas signaling mediates the neuronal apoptosis and motor side effects of GSK-3 inhibition in a mouse model of lithium therapy. *J Clin Invest* 2010; **120**(7)**:** 2432-2445.